COMPARISON, CHARACTERIZATION, AND INTERPRETATION OF GEOTHERMAL FLUID GEOCHEMISTRY IN THE SEDIMENTARY ENVIRONMENTS OF KIBIRO, PANYIMUR, AND ÖXARFJÖRDUR

Grace Lajwe
Ministry of Energy and Mineral Development
Department of Geological Survey and Mines
P.O. Box 9, Entebbe
UGANDA
gracelajwe@yahoo.com

ABSTRACT

Geochemical data interpretation of representative chemical, analytical, and isotopic results for geothermal waters and gas in sedimentary environments obtained by standard analytical methods were studied in this research work. Techniques like chemical geothermometers (silica and cation geothermometers) and gas geothermometers were used in predicting the variation in temperatures in three geothermal systems, i.e. Kibiro and Panyimur in the East Africa Rift System, and Öxarfjördur in Iceland. The speciation programme WATCH was used to calculate the activity of the different species of anions and cations, Na/K, Quartz and Chalcedony temperatures, a Ternary diagram for Na/1000-K/100-$\sqrt{Mg}$ based on the equilibration conditions for these cations in these waters at particular temperatures, and a Cl-SO_4-HCO_3 ternary plot were constructed. Different mixing models and plots of different constituent relationships were used in the comparison, characterization and interpretation of the geochemistry of these different geothermal areas. The geochemistry of magmatically driven geothermal systems may be used to develop effective exploration techniques for the geothermal systems that are driven by temperature gradients like the East African Rift System (EARS), the western branch of which Kibiro and Panyimur are part.

The chemical and isotopic composition of the water samples from Kibiro, Panyimur and Öxarfjördur, suggest mixing of cold groundwater with geothermal waters. Major ions and isotope parameters were used to characterize the waters from Kibiro and Panyimur as Na-Cl-HCO_3 waters, and water from Öxarfjördur as Na-Cl water. The main processes affecting the geothermal system in the sedimentary geological environment are: dilution and conductive cooling.

1. INTRODUCTION

For future exploration, building a conceptual model, and deciding on the utilization of geothermal resources in the area where they exist, a sound understanding of the chemistry of the geothermal fluids needs to be established in the beginning of the exploration phase for better facilitation and approaches

(Bruhn et al., 2010). Water and gas chemistry have been used for the last decades to: find the origin of the geothermal fluids, understand the mixing effects in the geothermal system, evaluate subsurface temperature, and predict corrosion and scaling problems during the use of these fluids (Fournier, 1977; Rybach, and Muffler, 1981; Arnórsson, et al., 1983; Arnórsson, 2000; Giggenbach, 1988).

The chemical composition of geothermal steam and water from natural manifestations provides initial constraints on reservoir temperature, and helps identify production properties and potential environmental concerns related to the utilization of the geothermal fluid. These can only be attained by carrying out geochemical exploration, one of the exploration techniques applied in the search for any geothermal resource for any utilization.

This project aims to investigate the geochemical relationship of the geothermal waters of Kibiro and Panyimur geothermal areas in East Africa and compare them with the low temperature geothermal system of the Öxarfjördur geothermal field which is located in North Iceland. The formation conditions of the geothermal fluids differ from one area to another (Hjartarson et al., 2005); this can only be proven by analysing the chemical characteristics and comparing the findings with the different formation conditions. The geology of these geothermal areas is briefly described, together with a classification of the geothermal waters. The speciation program WATCH (Bjarnason, 2010), and geothermometers were mainly used for the determination of the reservoir temperatures and equilibrium conditions.

Geothermal systems all over the world are mostly associated with a rift system where a powerful heat source is close to the surface of the earth (Björnsson et al., 2005). The geothermal activity in Kibiro and Panyimur is largely restricted to the rift system (Figure 1) of the western branch of the EARS, with geothermal manifestations like fumaroles, hot springs and travertine occurring along some of the border faults of the rift valley and within the volcanic fields (Data and Bahati, 2003). The geothermal system of the Öxarfjördur area in north Iceland is also within a major graben which is associated with current volcanic activity.

1.1 Objectives of the study

There are two objectives: 1) to understand the geochemical evolution of geothermal waters in two different sedimentary geological environments by carrying out a classification and an interpretation of their geochemical analytical results; 2) to develop better geothermal exploration and exploitation methods and techniques for geothermal waters occurring in sedimentary environments.

2. LITERATURE REVIEW

2.1 Geology of the Western branch of the East African Rift System

The western arm of the EARS, where the Kibiro and Panyimur areas of this study are located, has Cenozoic rift faults (Atekwana et al., 2004) starting from the north along the Sudan border, and then curving to the west and southwest along the border with the Democratic Republic of Congo, and south to Rwanda and Burundi for about 100 km. The western branch of the EARS is considered to be at an early stage of development, and is younger, that is Late Miocene to Recent, than the more mature eastern branch (Morley, 1999). The rifting region has a higher heat flow than the surrounding Pre-Cambrian terrain. Two different *en echelon* strands are found in the Western Rift, separated by the Rwenzori Mountains which rise from a base of less than 1000 m in the Rift to over 5000 m elevation. Within the rift valley there are thick layers of late Tertiary and Quaternary sediments, fresh water and saline crater lakes, volcanics, and plutonic bodies identified beneath L. Albert and L. Edward (EDICON, 1984). The majority of the geothermal areas of Uganda are found in the Western Rift Valley (Figure 1).

The western branch of the rift runs along the western side of Lake Victoria and along the edge of the East African plateau (Figure 1). The geography of the western branch is typically half grabens characterized by high angle normal rift faults. The rift is characterized by a paucity of volcanism relative to the Kenyan and Ethiopian rifts (Ebinger et al., 1989). The Lake Albert Rift was initiated in early Miocene and is dominated by a thick sequence of sediments. It is characterized by an abundance of potassic alkaline rocks that consist of basalts, carbonatites, ultrapotas- sic mafic rocks and potassic mafic-felsic lava.
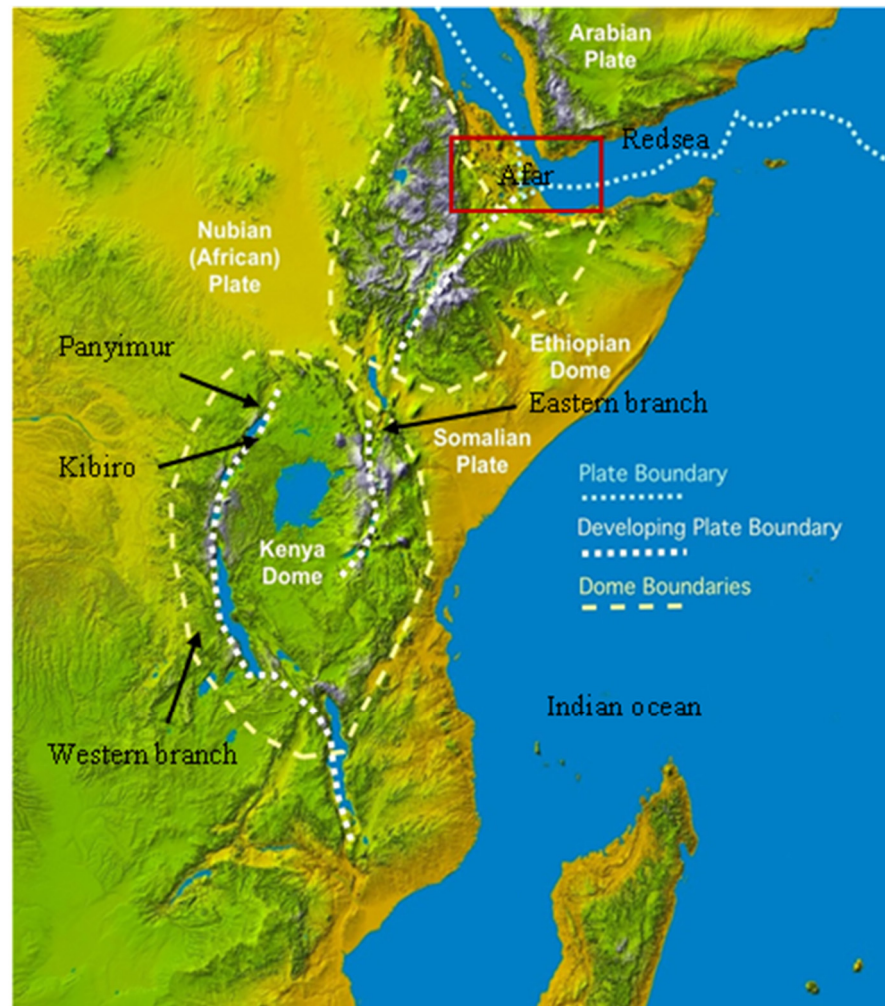

FIGURE 1: Modified EARS (Wood and Guth, 2012)

2.1.1 Geology of Kibiro

The area (Appendix I) has some volcanic rocks injected through Pleistocene lacustrine rocks in the rift valley and granitic gneisses on and above the escarpment at Kibiro; big dykes of basic intrusive rocks can be traced in some cases for miles in the argillites and gneisses trending NNE to SSW. The mineralogical composition of the rocks in this area is: porphyritic augites, pyroxexes, ilmenite, and titaniferous minerals. In addition to the more basic intrusives, there are also other granitic types like charnockites found 4.8 km southeast of Kibiro in a very large intrusion running east and west, presumed to be a late date intrusion related to faults (Kato, 2003).

The geology of the Kibiro geothermal area (Figure 2) is quite unique in its tectonic setting (Gíslason et al., 2005). Geological and geophysical studies carried out in this area revealed that the geothermal activities may be associated with the block faulted granites some distance from the main rift system.

2.1.2 Geology of Panyimur

The area (Appendix I) is characterized by fractured crystalline basement rocks such as coarse hornblende gneisses, coarse hornblende garnet rocks, talcose rocks and pegmatitic veins in a gorge that dips into the escarpment. In the area there is foliation/basement schistose trending- NNE-SSW. In addition, there is another schistose trend almost NE, parallel to the major local faults (Natukunda, 2013). The major rocks in the area include crystalline basement rocks, which are coarsely jointed granitic-gneiss with outcrops to the west and Pleistocene sediments to the east of the Rift fault boundary. There are some mylonite gneisses which are intruded by pegmatitic dykes, quartz veins and garnetiferous amphibolite dykes on

the escarpment, with the minor faults cross cutting the rift faults (upper Panyimur fault and the lower Panyimur fault, both striking northeast).

2.2 Geology of Öxarfjördur

The Öxarfjördur area in NE-Iceland is characterized by historical lavas of younger to older age, with thick sediment of about 1000 m (Georgsson et al., 2000) from a glacial river and by fissure swarms from active central volcanoes further inland (Figure 2). It is located at the junction between the NE-SW spreading zone which crosses Iceland, and a right – lateral transform zone, the Tjörnes Fracture Zone (Ólafsson, et al., 1993). Today the waters around the island are oxygen saturated. This could be due to the fact that major climate changes during the Pleistocene could have changed the paths of ocean currents and maybe that of the oxygen cycle, too.

The Öxarfjördur sedimentary graben falls in a transform zone of lateral transform movement, spreading, and volcanism in the zone between the North Iceland Volcanic Zone in Öxarfjördur and the spreading axis along the Kolbeinsey Ridge, (Jónsson et al., 1991).

The geological model of the Öxarfjördur sedimentary trough, based on the tectonic settings and geophysical data, indicates that it is younger than 1 Ma, with a probable thickness of up to 1 km at the shore inside the Krafla and Theistareykir fissure swarms, while thinning southwards where the sediments are expected to be more frequently interbedded with lavas and hyaloclastites (Georgsson et al., 2000).
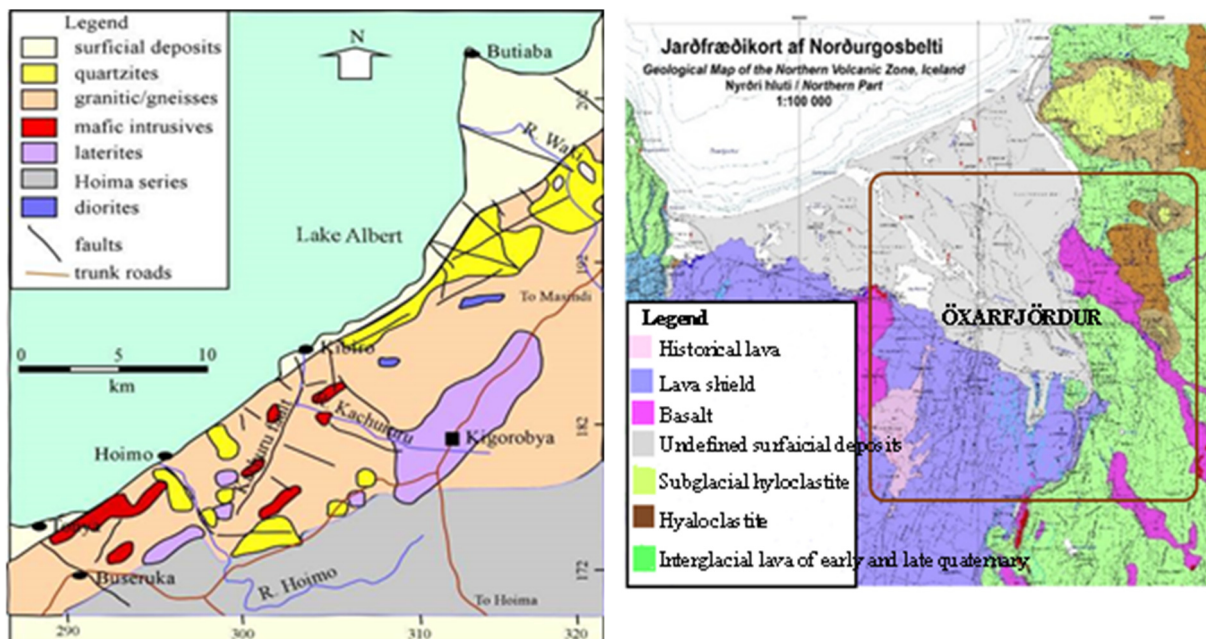

FIGURE 2: Geological maps of Kibiro and Öxarfjördur (DGSM, 2013 and ISOR)

2.3 Surface geothermal manifestations in Kibiro, Panyimur and Öxarfjördur

2.3.1 Surface geothermal manifestations in Kibiro and Panyimur

The hot springs in the Panyimur geothermal area are located within a stretch about 1.5 km along the main fault (Data and Bahati, 2003) and all are aligned in a northeast direction in the western escarpment of the Rift Valley, which probably means that they are controlled by the intersection of the traverse fault

together with the main rift. In addition to that, deposits of travertine, sulphurous algae, the smell of hydrogen sulphide and all the discharges are characterized by gas bubbling (Bahati, 2007).

The manifestations of Kibiro are mainly concentrated at Kibiro and Kachuguru, west of the escarpment, on the shores of Lake Albert; some fumarolic activity can be seen at Kachuru and along the escarpment for approximately 1.5 km from the intersection of the Kachuguru fault and the main escarpment to the Kibiro hot springs (Bahati, 2012). There are some calcite deposits observed in cracks and fissures in many locations along the escarpment, the Kachuguru fault, the Kitawe fault and in the crystalline rocks located south-southeast of Kibiro, indicating extinct thermal fluid discharges. The hot springs at Kibiro are apparently related to a secondary fault, oblique to the main Rift fault, and most likely controlled by their intersection (Figure 2). The total flow measured from the hot springs is approximately 7 l/s and the maximum surface temperature is 86.4°C (Gíslason et. al., 1994).

2.3.2 Surface geothermal manifestations in Öxarfjördur

The surface geothermal manifestations in the Öxarfjördur region are meagre, mainly in the form of warm springs and warm ground within the active fissure swarms. Geothermal manifestations are known at 13 locations, which can be divided into 3 groups (Georgsson et al., 1993). These groups are: 1) The Krafla fissure swarm which has the most important sites like Skógalón where water at a shallow level has temperatures up to 100°C, covering an area of several hundred square metres, and Bakkahlaup with warm ground covering a wide area with temperatures of up to 80°C in the uppermost part, considerably lower before the Krafla fires. 2) The Theistareykir fissure swarm in the western part of the Öxarfjördur area, with the most important one at Ytra Lón close to the coast, with recently measured temperatures of 50°C; older records show temperatures above 80°C. 3) Geothermal sites found outside the active fissure swarms.

2.4 The chemistry of the geothermal fluids

2.4.1 Brief overview of geothermal fluid chemistry

The chemistry of geothermal fluids is diverse and largely reflects the geological setting of a particular area (Henley and Ellis, 1983). Most of these chemical differences depend upon the source of recharge waters with some contribution of gases from magmatic or metamorphic sources. Geothermal fluids contain a number of different constituents with varying concentrations (Ármannsson, 2013), with important chemical parameters which characterize geothermal fluids, such as pH which describes the acidity or alkalinity of the fluid, and TDS which gives a measure of the amount of chemical constituents dissolved in the fluids.

The constituents of geothermal water can be grouped into two categories with respect to their properties, i.e.:

1) Reactive constituents, which are also used as geo-indicators due to the fact that they tend to equilibrate with some of the minerals in the geothermal system (Arnórsson, 2000a). Information on temperature and the steam fraction, which together constitute the physical state of the geothermal system, may be provided by these constituents.
2) Conservative constituents such as Br, Cl, B, N_2, ^2H, ^{13}C, ^{40}Ar, and ^{18}O (Arnórsson, 2000a) may be used to trace the origin and flow of the geothermal fluids, as they do not take part in water-rock interaction.

The geothermal fluids or natural waters may be classified using the Cl-SO_4-HCO_3 ternary plot diagram (Giggenbach, 1991). This diagram is used to distinguish a number of different types of thermal waters like: immature unstable waters, giving an indication of the mixing relationships or the geological groupings; steam heated waters; volcanic waters; and peripheral waters. And this leads to the provision

of a trend and preliminary statistical evaluation of the grouping of geothermal waters (Giggenbach, 1988). Water circulating in high-enthalpy geothermal reservoirs is mostly of meteoric origin but, in some geothermal systems, it may be oceanic or evolved connate waters (Bruhn et al., 2010). For geothermal systems which are located along the convergent plate boundaries and are close to the volcanic-magmatic association, the deep magmatic heat source tends to add some acidic gases like CO_2, SO_2, HF, H_2S and HCl, with some andesitic waters in the system.

In high-enthalpy geothermal systems, four different types of geothermal waters have been classified (Truesdell, 1991; Giggenbach, 1988; Henley et al., 1984; Ellis and Mahon, 1977):

1) Acid sulphate water: this is the type of thermal water which is mainly found in the upflow part of the geothermal system, (Bruhnet al., 2010). This type of geothermal water is characterized by a low pH of 0 to 3 and a low concentration of chloride. It reacts very fast with the host rocks, mainly giving advanced argillic alteration paragenesis. Composed of alunite and kaolinite. CO_2 and H_2S are the two main types of gases in this geothermal environment. The H_2S may undergo oxidization in the upflow zone to form SO_4 near the surface and contains constituents mostly dissolved from the surrounding rock with which it is in contact **(**Ármannsson, 2009).

2) Sodium – chloride water: water with a chloride concentration of up to 10,000 mg/kg, and pH of approximately ±1 or ±2 units to a neutral pH at depth, for example 5.5-5.6 at a temperature of 200ºC to 300ºC. This type of water contains the following constituents in higher concentrations than in cold water: Na, B, F, Li, Si, K, Ca, but with low Mg and with CO_2 and H_2S as the main dissolved gases (Bruhn et al., 2010).

3) Acid chloride – sulphate water: this type of water is found in the deepest part of the connecting neutral pH that is a NaCl system, there and in the inflow of magmatic gases rich in sulphur and hydrochloride species, namely H_2S and SO_2; this produces a very reactive aqueous solution that dissolves the rock or leaches the cations from them, leading to the deposition of pyrite, alunite, kaolinite and anhydrite (look at the chapter in Ármannsson, 2010). The acid Chloride – Sulphate water is mainly found in crater lakes (Bruhn et al., 2010). The interaction of the magmatic gases with rock masses and water is greater at depth, with higher temperatures and lasts for a longer period than in the crater lakes. This leads to the formation of neutral NaCl waters (Reed, 1991; Giggenbach, 1997), due to more neutralization in the system.

4) Sodium bicarbonate water: found in: the zone of condensation for a vapour-dominated geothermal reservoir; the marginal regions of the liquid-dominated geothermal reservoirs; in the deep geothermal reservoir located in sedimentary rocks and/or metamorphic rocks. The condensation of geothermal steam in a free oxygen groundwater in a relatively deep zone may be the dissolution of CO_2, present in some of the gases in the system, which can lead to the origin of bicarbonate rich waters (Bruhn al., 2010). The lack of oxygen in this system prevents the oxidation of H_2S, meaning that the acidity in the aqueous solution is from the dissociation of the H_2CO_3 as shown in Equation 1.

$$H_2CO_{3(aq)} \quad \rightleftharpoons \quad CO_{2(g)} \ + \ H_2O_{(l)} \tag{1}$$
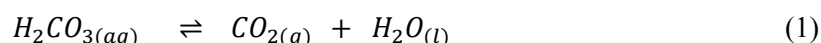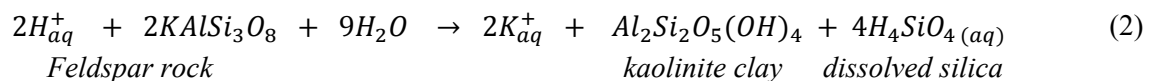
The conversion of feldspars to clay is aided by this weak acid, especially in medium to high temperature geothermal reservoirs, gives rise to neutral aqueous solutions.

2.4.2 Water-rock interaction

Geological processes are mostly a result of reactions which take place between the minerals in the rock and the fluids (Driesner, 2013). When geothermal water or fluids move through the rock, they may chemically react with the rock with which they come into contact, (and some of the rocks themselves are chemically complex). This may lead to the following: 1) dissolution of some selective minerals

from the rock; 2) Precipitation of some minerals from the solution; and 3) substitution of certain chemical elements in the fluids by other elements in the minerals. All three processes may lead to secondary mineral formation by depletion or enrichment of some of the chemical components from the fluids (Rodríguez, 2011), or removal of chemical components from the rock due to the dissolution of the primary minerals. A series of chemical reactions, associated with the interactions between the water, the chamber rock and the path by which the water reaches the earth's surface (Arnórsson et al., 2007) may occur, for example reactions which typically involve sulphur and /or metal cations. Water - rock interactions generally take place slowly, that is primary rock dissolves very slowly in water but, like most reactions, the process is faster at higher temperatures. The changes in the chemical and/or mineralogical composition may or may not lead to volume changes in the rock (Arnórsson et al., 2002). If the volume of the rock is changed, then porosity and permeability may be affected, too. When the reaction between water and rock is prolonged, some of the ionic species and saturated silica are dissolved (Equation 2). $Na^+(aq)$ and $Ca^{2+}_{(aq)}$ also dissolve in the geothermal water.

Physico-chemical conditions like temperature may, if decreased, lead to the precipitation of minerals due to low solubility (Equation 4). Boiling, upon pressure decreases, may cause re-partitioning of the forces between the vapour and the liquid phase leading to solubility decreases for some metals, for example, gold.

$$2H^+_{aq} + 2KAlSi_3O_8 + 9H_2O \rightarrow 2K^+_{aq} + Al_2Si_2O_5(OH)_4 + 4H_4SiO_{4\,(aq)} \qquad (2)$$
$$\textit{Feldspar rock} \qquad\qquad\qquad \textit{kaolinite clay} \quad \textit{dissolved silica}$$
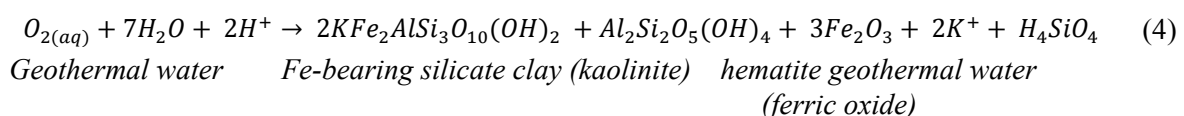
Water may be in equilibrium with the rock for sufficiently long to be used to calculate the temperature of the water. In effect, the ratios of the concentrations of the liberated cations like: Ca^{2+}, Na^+, Mg^{2+} and K^+ are temperature dependent. The most important process governing their relative contents is rock dissolution and equilibration (Giggenbach, 1984).

The solubility of silica is also temperature dependent, but this equilibrium is attained rather more rapidly than the dissolution of most other silicate minerals.

$$H_4SiO_{4(aq)} + 2H_2O \rightarrow SiO_2 \qquad (3)$$
$$\textit{Dissolved silica} \qquad\qquad \textit{siliceous sinter}$$
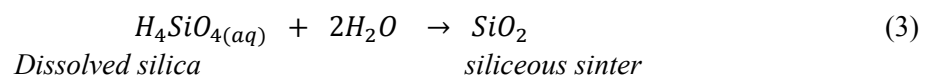
This reaction may be used as the basis of a geothermometer (Afeworki, 2010). Any difference in temperatures obtained from the two geothermometers is related to the sampling of the water relative to the deep aquifer: waters that have moved away from the aquifer are likely to have lower temperatures derived from silica concentrations than temperatures derived from concentrations of Na, K and Ca. This may either be due to faster equilibration in the silica dissolution than the ion-exchange reactions or to mixing with dilute water. Some ion exchange reactions are, however, very fast such as the K-Mg reaction, and a geothermometer based on it may even show a lower temperature than a silica geothermometer.

Iron and manganese ions may be liberated from silicate minerals and ultimately precipitate as their highly coloured oxides. The example below shows the oxidative liberation of iron from a silicate mineral under acid conditions. Iron (II) is oxidized to iron (III).

$$O_{2(aq)} + 7H_2O + 2H^+ \rightarrow 2KFe_2AlSi_3O_{10}(OH)_2 + Al_2Si_2O_5(OH)_4 + 3Fe_2O_3 + 2K^+ + H_4SiO_4 \qquad (4)$$
$$\textit{Geothermal water} \qquad \textit{Fe-bearing silicate clay (kaolinite)} \quad \textit{hematite geothermal water}$$
$$\textit{(ferric oxide)}$$

As the water rises to the surface it cools, and silica minerals are precipitated along with other minerals. This may help "cap" the aquifer, and prolong the geothermal system's existence. Water that does reach

the surface through faults and fractures will cool further and produce the sinter mounds and terraces that are typical around geysers and hot springs.

When water in a geothermal system has attained a high temperature that is above 100°C, it will react with the rock to a greater extent, leading to the production of significant oxygen shift, which can be proven by Equation 4 (Arnórsson, 2000b); this may tell us if the geothermal water shows precipitation which fell during the present day climate or under different climatic conditions.

2.4.3 Mixing in the upflow zones

Geothermal waters may be mixed with cold water after a certain period of conductive cooling of the hot water, before, after or during boiling (Arnórsson, 2000b). Depending on pressure and temperature conditions, the main component of geothermal fluids, H_2O, can be present in different physical states (Bruhn et al., 2010). The presence of a single liquid phase in the geothermal reservoir is the most frequent situation, but it is not the only one, since either a two-phase liquid vapour mixture or a single vapour phase can be present in the reservoir. These possibilities can be ascertained by accurate enthalpy data or by gas geochemistry (Giggenbach, 1980; Bertrami et al., 1985).
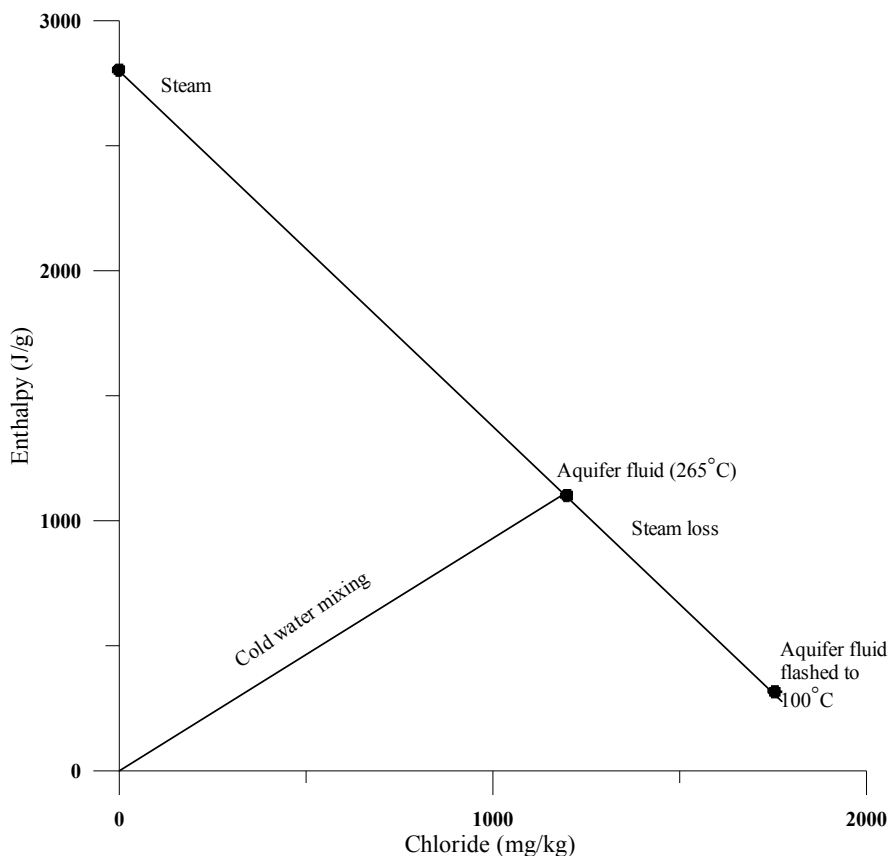

Large variations in the temperature and flow rates of thermal springs in a particular field that can be linked with the parallel variations in the concentrations of the non-reactive components in the water, like Cl, usually constitute the best evidence that mixing has taken place (Marini and Cioni, 1985). Mixing models have been developed to allow the estimation of the hot water component in mixed waters emerging in springs or discharged from shallow drill holes (Truesdell and Fournier, 1977). Three mixing models are most frequently applied: 1) the chloride-enthalpy model; 2) the silica-enthalpy mixing model; and 3) the silica – carbonate mixing model.

FIGURE 3: Enthalpy versus chloride for boiling and dilution (Foumier, 1979)

The enthalpy versus chloride plot is a suitable tool for distinguishing the effects of boiling (steam loss) and mixing, since both steam and cold waters, which generally have low chloride contents, are characterized by very different enthalpy values (Fournier, 1979). The enthalpy-chloride plot (Figure 3) shows that boiling moves the liquid from the point representative of the 265°C geothermal liquid towards higher chloride contents and lower enthalpies, whereas the addition of cold, dilute waters causes a decrease in both enthalpy and chloride. If the discharged water is cooled, mainly through conductive heat loss, the chloride concentration of the deep hot water remains unchanged (Bruhn et al., 2010).

The linear relationship between the concentrations of conservative components like CI and B or CI and δ^2H are generally considered to constitute the best evidence for mixing (Bruhn et al., 2010). The magnitude of the oxygen shift depends on the extent of the water - rock interaction. Generally, increasing temperature enhances chemical reaction rates (Stefánsson, et al., 2007) including reactions involving water and rock, hence increasing the ^{18}O isotope shift (see Chapter 2.4.5). Mixing of geothermal waters with local groundwater may manifest itself in a linear relationship between the δ values for ^2H and ^{18}O or between these values and the aqueous concentrations of conservative elements such as Cl.

Hot water ascending to the surface from the geothermal reservoir tends to have a relatively high concentration of total dissolved solids (Árnason and Gíslason, 2009), but cold groundwater contains relatively low total dissolved solids, so if such cold groundwater mixes with the hot water, it leads to dilution which reduces the concentration of the total dissolved solids (Rodríguez, 2011). Chloride, which is a non-reactive component in water, tends to give the best evidence of mixing in water systems, depending on the variation of temperature and the flow rates of the geothermal hot or cold water.

In many geothermal hot springs, mixing of the hot and cold water leads to dilution and cooling (Noda and Shimada, 1993); to prove this by using the different mixing model techniques, the chemical composition of each component in the geothermal water needs to be evaluated thoroughly. And for better use of mixing models, to establish whether there is mixing in the up flow zone of a geothermal system, a large number of samples from the geothermal area is required. The chloride enthalpy plot is used in mixing prediction because chloride concentration increases gradually with continuous rock dissolution with an increase in temperature (Yohannes, 2004).

2.4.4 Mineral saturation

This is one of the techniques used in the evaluation of mineral equilibrium, using the assumption of mineral dissolution in solution, taking into account the different physical conditions in which this mineral dissolves (Arnórsson and Bjarnason, 2007). Determining the chemical equilibrium between the aqueous solution and the mineral in any natural system needs to be carried out with an idea of the activities of the different species present in that solution (Arnórsson et al., 2002).

2.4.5 Isotope chemistry of geothermal fluids

Isotopic chemistry is one of the most important tools used in the exploration for geothermal resources today. To gain representative results for a particular geothermal system, the isotope values need to be interpreted in conjunction with other chemical techniques (Giggenbach et al., 1984; Giggenbach., 1991; Craig., 1963). It is used mainly to establish the isotopic characteristics (that is $\delta^{18}O$ and δ^2H) of the precipitation in relation to the altitude and latitude, together with continental effects. There is a general decrease in the values of the $\delta^{18}O$ and δ^2H for samples collected from geothermal areas that are further inland, at a higher elevation and at higher latitudes. And these values are more closely related to the meteoric water line through the equation:

$$\delta^2H \;=\; 8\,\delta^{18}O + d \tag{5}$$

where d = 10 and for each isotope $\delta = [(R_{sample} - R_{SMOW})/R_{SMOW}] \times 1000,$ reported in ‰, and R = the ratio of the number of atoms of a given isotope to the number of atoms of the element's most abundant isotope, i.e. $R = {^{18}O}/{^{16}O}$ for oxygen-18 and $R = {^2H}/{^1H}$ for deuterium and SMOW is the Standard Mean Ocean Water as defined by the IAEA.

In a high-temperature geothermal system, there may be isotopic exchange between rock minerals which are rich in $\delta^{18}O$ and water, causing the $\delta^{18}O$ values to increase and fall to the right of the world meteoric line, or the so called oxygen isotope shift (Giggenbach, 1991). Along the convergent plate boundaries of a volcanic system, Giggenbach (1992) showed that there is a linear relationship between the values of $\delta^{18}O$ and δ^2H, which is also the case in numerous geothermal systems showing a mixing trend in

common with a magmatic source with δ^2H of about -20 ± 10‰ and $\delta^{18}O$ of about +10 ‰. This phenomenon is common in subduction systems and explains the isotope signature of andesitic waters, but is unlikely to be applicable in the systems presently studied.

2.4.6 Geothermometers in geothermal exploration

This has proved to be one of the major exploration tools used in the search for geothermal energy. This method is based on the isotopic and the chemical composition of the fluids that discharge from natural hot springs, cold springs and wells (D´Amore and Arnórsson, 2000b). They are used for the following: 1) to predict or estimate the subsurface temperature of the geothermal system which is expected to be encountered in case of any drilling in the area for exploration or production purposes; 2) during the late stages of geothermal development and utilization, especially in establishing the horizons in productive wells; and 3) the chemical state of the recharging water in the vicinity of a well as a result of cooling or boiling, due to depressurization, can be determined by this technique (Bruhn et al., 2010).

In a geothermal system, most of the chemical reactions are temperature dependent (Ármannsson, 2009) and their kinetics are not fast at a relatively low temperature, hence the equilibrium characteristics are preserved even when the water flows to the surface and cools down. Using the assumption of the conservation of mass and heat and determining the chemical composition of the surface geothermal fluid, the subsurface temperature may be determined.

Geothermometers are divided into basically three categories:

1. Isotope geothermometers
These are based on the fractionation of the isotopes of light elements (given by Equation 5) between gaseous and aqueous portions of the geothermal fluids. This is mainly temperature dependent making it very important:

$$1000 In\ \alpha_{AB} = \delta_A - \delta_B \tag{6}$$

where $ln\ \alpha AB$ = Isotopic fractionation in two phases;
   δ_A = Concentration of constituent A;
   δ_B = Concentration of constituent B.

2. Water or solute geothermometers
These are based on the fact that the concentration and any ion ratio for an aqueous species may be used as a geothermometer, taking into consideration that equilibration is attained for the reaction (Arnórsson and Svavarsson, 1985). The most common types of such geothermometers are the silica (quartz and chalcedony), the Na–K and the Na–K–Ca (Fournier, 1973; Fournier and Truesdell, 1973; Ellis and Mahon, 1977; D'Amore and Arnórsson, 2000). For this particular research work, the water or solute geothermometers used are shown by the equations below.

Arnórsson et al., 1983 (Cation):

$$T(°C) = \frac{933}{0.993 + \log\left(\frac{Na}{K}\right)} - 273.13 \tag{7}$$

Truesdell and Fournier, 1976 (Cation):

$$T(°C) = \frac{856}{0.857 + \log\left(\frac{Na}{K}\right)} - 273.13 \tag{8}$$

Giggenbach et al., 1994 (Quartz):

$$T(\text{°C}) = \frac{4410}{14.0 + log\left(\frac{K^2}{Mg}\right)} - 273.13 \tag{9}$$

Fournier, 1977 (Quartz):

$$T(\text{°C}) = \frac{1522}{5.75 - logS} - 273.13 \tag{10}$$

Fournier, 1977 (Quartz):

$$T(\text{°C}) = \frac{1309}{5.19 - logS} - 273.13 \tag{11}$$

Arnórsson et al., 1983 (Quartz):

$$T(\text{°C}) = \frac{1112}{4.91 - logS} - 273.13 \tag{12}$$

Fournier, 1977 (Quartz):

$$T(\text{°C}) = \frac{1032}{4.69 - logS} - 273.13 \tag{13}$$

Fournier and Truesdell, 1973 (Cation):

$$T(\text{°C}) = \frac{1647}{log\frac{Na}{K} + \beta\left[log\left(\frac{\sqrt{Ca}}{Na}\right) + 2.06\right] + 2.47} - 273.13 \tag{14}$$

Arnórsson, 2000 (Quartz):

$$T(\text{°C}) = -55.3 + 0.36590S - 5.3954 \times 10^{-4}S^2 + 5.5132 \times 10^{-7}S^3 + 74.360 \tag{15}$$

Fournier and Plotter, 1982 (Quartz):

$$T(\text{°C}) = -53.5 + 0.11236S - 0.5559 \times 10^{-4}S^2 + 0.1772 \times 10^{-7}S^3 + 88.390 \log S \tag{16}$$

Arnórsson, 2000 (Quartz):

$$T(\text{°C}) = -66.9 + 0.13780S - 4.9727 \times 10^{-5}S^2 + 5.5132 \times 10^{-8}S^3 + 87.841 \log S \tag{17}$$

Verma and Santayo, 1997 (Quartz):

$$T(\text{°C}) = -44.119 + 0.24469S - 1.7414 \times 10^{-4}S^2 + 79.305 \log S \tag{18}$$

$$Na - feldspar + K^+ = K - feldspar + Na^+ \tag{19}$$

$$2.8\,K - feldspar + 1.6\,water + Mg^{2+}$$
$$= 0.8\,K - mica + 0.2\,chlorite + 5.4\,silica + 2\,K^+ \tag{20}$$

$$T_{K-Mg} = 4410par + K^+ = K - feldspar + Na^+ \tag{21}$$

3. Gas geothermometers

These are applicable for gas and steam samples since in many geothermal fields there are fumaroles, hot ground and acidic surface waters. These types of geothermometers are grouped into three as follows:

1) The mineral gas equilibria geothermometers;
2) Gas – gas equilibria geothermometers; and
3) Mineral – gas equilibria geothermometers involving CO_2, CH_4 and H_2S, which need to be externally fixed, using empirical methods.

3. METHODS

3.1 Data sources

The geochemical data of selected hot springs used in this research work were collected from the department of geological survey and mines in Uganda, (GSMD). These data were acquired during the UNDP/UNDESD project funded by OPEC and the Iceland Government, and data for the Öxarfjördur area were collected from Iceland GeoSurvey, (ISOR), by the geochemistry department; these results were acquired as part of the early studies for the search for oil. The data set includes analysed samples from selected hot springs, a cold spring and wells listed in Table 1.

3.2 Field sampling methodology

In all these areas of research work, geochemical sampling of the hot springs, and the wells was carried out by the GSMD geochemistry team, together with Dr. Halldór Ármannsson from the Iceland GeoSurvey, in Uganda (GSMD, 2008), while the sampling from the Öxarfjördur area, north Iceland, was carried out by the Iceland GeoSurvey geochemistry team. Measurements of the physical parameters and an analysis of the volatile components of the water samples collected were carried out in the field. Rock samples were collected for mineralogy analysis to determine the source of salinity in the geothermal waters from Kibiro and Öxarfjördur, although these were not used in this research work.

Untreated samples were collected for pH, carbonate, H_2S and conductivity measurements and also for the analysis of Mg and SiO_2. During the sampling, the concentrations of SiO_2 were expected to be more than 100 ppm, so the samples were diluted with distilled or deionized water to bring the concentrations into the range of 30 to 100 ppm in triplicate and the dilution factor was recorded. Samples were also collected and anions were filtered; for the cations, the filtered samples were acidified with nitric acid. All the samples used in the determination of sulphate were precipitated with $Zn (CH_3COO)_2$ and then the sulphate was analysed after filtration of the samples. For the analysis of stable isotopes (δ^2H, $\delta^{18}O$), the isotope laboratory needed 60 ml of filtered sample. A summary of the sample treatment is given in Table 2 and the preservation method for the sampling of hot spring and hot water wells are presented in Table 3.

These samples had to be preserved both by chemical and physical processes, as shown in Table 3, in order to ensure no changes in the chemical and physical characteristics of these waters and the gases. Preservation techniques were carried out both in the field and in the laboratory, depending on the handling of the different constituents in these samples.

TABLE 1: Chemical composition (mg/kg) of selected samples from the Öxarfjördur, Kibiro and Panyimur and (isotope values in ‰ SMOW)

LOC	T(°C)	PH	CO2	H2S	NH3	Cl	SO4	F	Br	Na	K	Ca	Mg	Al	Fe	SiO2	B	Li	TDS	δ^2H	δ^{18}O
ÖXA																					
ISK	95.7	7.mar	30.mar	0.06	0.00	3539	232	0.41	12.jan	1818	98	400	jul.14	0.00	0.00	148	jan.77	0.00	6401	-87.8	-9.3
ISG	92.0	8.jul	30.jun	0.05	0.00	1807	85.9	0.33	6.feb	950	55	186	0.07	0.00	0.00	123	jan.40	0.00	3326	-88.5	-9.6
IBK	78.5	8.apr	30.agú	<0.05	0.00	658	46.1	0.59	2.feb	427	41	17	jan.47	0.00	0.00	100	0.53	0.00	1283	-90.0	-12.0
IA1	98.0	9.mai	12.apr	<0.05	0.00	2460	138	0.65	<0.0	1250	77	259	0.18	0.00	0.00	139	<0.0	0.00	4630	0.0	-10.0
IA3	96.0	7.sep	24.mar	0.07	0.00	1534	96.6	0.27	5.mar	833	44	154	0.42	0.00	0.00	129	1.00	0.00	2709	-100.4	-10.9
IA4	132.0	8.jún	5.jan	<0.03	0.00	2110	150	0.12	agú.23	1222	67	185	0.65	0.00	0.00	214	jan.36	0.00	4085	-114.1	-11.1
IJÖ	2.sep	7.agú	42.1	<0.03	0.00	6.sep	7.sep	0.16	<0.0	19.agú	1.apr	6.jan	mar.62	0.00	0.00	16.ágú	<0.0	0.00	104	-98.7	-13.9
ISW	4.0	8.jan	105	<0.03	0.00	18288	2545	0.70	<0.0	10113	396	378	1162	0.00	0.00	1.jún	<0.0	0.00	36110	-7.1	-0.8
KIB																					
KM1	86.5	7.jún	146	10.apr	0.00	2500	46.6	5.des	16.júl	1530	169	62.0	8.jan	0.037	0.00	129	feb.26	1.500	4576	-11.3	-2.01
KM2	81.1	júl.14	155	13.0	0.00	2450	26.apr	5.feb	16.apr	1490	164	62.9	júl.96	0.041	0.02	125	feb.23	1.480	4436	-11.8	-2.08
KM3	71.8	júl.14	155	17.mar	0.00	2440	15.apr	apr.74	16.feb	1480	165	66	sep.21	0.044	0.00	122	feb.21	1.460	4384	-10.6	-1.98
KM4	39.5	8.mai	115	<0.0	0.00	2580	49.9	mai.37	17.mar	1570	182	76	agú.71	0.029	0.03	135	feb.47	1.530	4548	-3.9	-1.01
KM4	29.agú	jún.89	367	<0.0	0.00	31.2	139	0.37	0.26	87.5	7.júl	76	39.5	0.010	jan.50	90.5	<0.0	0.02	662	-15.2	-3.58
KM6	23.jún	jún.26	130	<0.0	0.00	5.feb	5.mar	0.12	0.04	12.apr	2.jún	15	8.mar	0.007	0.74	70.8	<0.0	0	124	-4.1	-1.57
KM7	24.sep	jún.72	232	<0.0	0.00	123	227	0.12	0.64	50.6	7.mai	138	39.5	0.014	0.72	76.1	<0.0	0.02	680	-5.2	-2.08
KM8	30	agú.93	236	<0.0	0.00	24.feb	19.mar	0.83	0.13	72.3	49	9.ágú	27.mar	0.015	0.07	0.5	<0.0	0.01	338	39.8	mai.47
PAN																					
PA1	58	agú.66	71	mai.61	2.jan	470	26	5.feb	1.mai	352	11	4.mai	0.36	0.47	0.1	73	0.65	0.12	890	-7.7	-3.5
PA2	45	agú.45	109	feb.48	1.jún	379	36	4.júl	0.93	321	9.mai	8.mai	0.68	0.17	0	69	0.58	0.00	794	-5.5	-3.3
PA3	35	júl.56	142	<0.0	0.25	83	19	2.apr	0.17	138	7.mar	8.apr	3.jan	0.21	0.2	54	0.22	0.00	337	1.sep	-2.5
PA4	49	9.jún	95.5	<0.0	0.12	53	4.apr	6.jún	0.29	110	2.jún	1.apr	0.04	0.17	0	70	<0.1	0.00	nd	-1.9	-2.5
PA5	48	agú.23	91.1	<0.0	<0.1	51	73	8.0	0.45	111	3.sep	6.jún	0.76	0.21	0.2	68	0.2	0.00	nd	2.mai	-2.0
PA6	60	agú.35	216	<0.0	<0.1	95	341	13.0	<0.2	322	18	24	2.júl	<0.1	0.1	118	0.18	0.19	815	-4.9	-18.8
PA7	42	agú.39	207	<0.0	<0.1	97	343	13.ágú	<0.2	323	19	21	1.mai	<0.1	0.2	129	<0.1	0.2	812	-4.8	-17.2
PA8	38	agú.44	207	<0.1	<0.1	96	352	13.0	<0.02	342	22	21	1.mai	<0.1	0.3	129	0.76	0.22	825	-16.6	-4.9

TABLE 2: Treatment and sub-samples from hot springs and hot water wells
(Ármannsson and Ólafsson, 2012)

Specification	Container	Capacity (ml)	Treatment	Used for
Ru	Glass	250-300	None; amber glass bottle with ground glass stopper	pH, CO_2, H_2S (if not in field) and conductivity
Ru	Plastic	200	None	Mg, SiO_2 if < 100ml
Rd (1:1)	Plastic	3×100	Dilution; 0ml of sample added to 50 ml of distilled, deionized water	SiO_2 if < 100ml
Fu	Plastic	200	Filtration	Anions
Fa	Plastic	200	Filtration; 0.8ml of conc. HNO3 acid added to 200 ml of sample	Cations
Fp, Fpi	Plastic	200, >500	Filtration; 2ml of 2M $ZnAc_2$ added to sample in 100 ml volumetric glass flask and ≥10 ml to ≥500 ml bottle containing ≥25mg SO4 to precipitate sulphide	SO_4, $\delta^{34}S$ and $\delta^{18}O$ in SO_4
Fui, Fuc, Fut	Glass	60, 1000	Filtration; 1, 60ml, and 2, 1000ml amber glass bottles	δ^2H, $\delta^{18}O$, ^{13}C and ^3H

Note: Fp =Filtered precipitated; Fpi =Filtered precipitated for isotope; Fui =Filtered untreated;
Fu =Filtered untreated; Fa =Filtered acidified; Ru =Raw untreated; Rd =Raw diluted.

TABLE 3: Preservation methods for geothermal samples (Ármannsson and Ólafsson, 2006)

Type	Method	Purpose	Used for
Physical	Filtration with 0.45 or 0.22 μ membrane filter	Prevent interaction with suspended matter	Anions, Cations, TDS
	Freezing	Prevent biological activity	Nutrients
	Airtight container	Prevent interaction with atmospheric air	
	On-site analysis	Prevent reactions of reactive constituents	Reactive constituents
Chemical	Base addition	Absorption of acid gases	CO_2, H_2S in steam, $\delta^{34}S$ in H_2S in vapour
	Acidification	Prevent adsorption on the walls of containers	Cations
	Precipitation	Prevent a constituent from reaction to change the concentration of another constituent	Sulphate to fix Sulphide
	Sterilization	Prevent biological activity, using HgCl or formaldehyde	
	Dilution	Prevent polymerization and precipitation	Silica
	Redox	To change oxidation state of volatile constituent to make it less volatile	Hg
	Ion exchange	Concentrate and further prevent adsorption on the walls of container of trace constituents	Trace cations
	Extraction	Concentrate and further prevent adsorption on the walls of container of trace constituents	Trace cations

3.3 Analytical methods

The Department of Geological Survey and Mines carried out the determination of the TDS and conductivity of the geothermal waters in their laboratory at Entebbe. The samples were then divided into different portions for analysis. Then the samples were sent for complete chemical analysis to the Institute of Geological and Nuclear Science, New Zealand (Ármannsson, 2010), but the samples collected from Öxarfjördur area were analysed in the Orkustofnun Laboratory. The methods and instruments summarized in Table 4 were used in the analysis of these samples.

TABLE 4: Analytical methods (Ármannsson and Ólafsson, 2006)

Constituents	Laboratory	Method	LOD	PR RSD%
Conductivity	GSMD	4 electrode		
pH	GSMD	GE		
CO_2 and H_2S	GSMD	Titration	0.02 – 1.0	3.8 – 13.7
SiO_2, B and NH_3	OS and GSMD	SP	0.01- 0.5	0.7 – 8.3
Na, K, Ca, Mg, Sr, Li	OS	AAS	0.0005-0.1	1.5 – 2.7
SO_4, Cl and Br	OS	IC	0.02 – 0.025	0.8 – 5.4
TDS	OS	GR	2.5	3.4
F	OS	ISE	0.05	0.9
Fe, Al and Mn	OS	FAAS	0.001	
$\delta^{18}O$ and δ^2H	USI	MS		
$CO_{2,\,n.c.}$, H_2S, n.c., CH_4, H_2, N_2, Ar, and C_2H_6	OS	GC	0.01 – 0.02	

4. RESULTS AND DISCUSSION

4.1 The aqueous chemistry of the geothermal fluids in these areas

The results for selected hot springs and hot water wells presented in Table 1 from Kibiro, Panyimur and Öxarfjördur are generally in the range of neutral – alkaline with pH of 6.7- 9.5. A general summary of the different chemical component ranges in the samples from Kibiro, Panyimur and Öxarfjördur are presented in Table 5. Samples from Öxarfjördur contain very low H_2S (<0.03 – 0.07 mg/kg), CO_2 (5.1 – 30.8 mg/kg); the $\delta^{18}O$ is -12 - -9.3 ‰, and δ^2H -114.1 - -87.8 ‰, and TDS is relatively high (1283 – 6401 mg/kg). Samples from Kibiro also contain relatively high CO_2 (115 – 367 mg/kg) and H_2S (0.0 – 17.3 mg/kg). Panyimur samples, in general, contain relatively low concentrations of all the chemical components. And, in general, the samples from Panyimur and Öxarfjördur contain lower concentrations of Mg than the samples from Kibiro. There is a relatively higher concentration of fluoride in some of the samples from Panyimur, compared to the samples from Kibiro and Öxarfjördur. The chemistry of these water samples differs mainly in the samples from Öxarfjördur which, in general, contain almost none or very little H_2S, but contain the highest amount of Na, K, TDS, and concentrations of SiO_2, Na, Cl, CO_2, Mg and TDS.

TABLE 5: Summary of the different constituents in mg/kg and stable isotopes
in ‰ SMOW of water samples of Öxarfjördur, Kibiro and Panyimur

	T(°C)	PH	CO₂	H₂S	Cl	SO₄
Gen	24 -132	6.26-9.5	5.1-367	<0.03-17.3	5.2-3539	1.9-352
Öxa	78.5-132	7.3-9.5	5.1-30.8	<0.03-0.07	658-3539	46.1-232
Kib	23.6-86.5	6.26-8.93	115-367	0-17.3	5.2-2580	5.3-227
Pan	35-60	7.56-9.06	71-216	<0.1-5.61	51-470	4.4-352
	K	**Ca**	**Mg**	**SiO₂**	**B**	**TDS**
Gen	2.6-169	1.4-400	0.07-39.5	54-214	<0.1-16.7	124-6401
Öxa	41-98	6.1-400	0.18-1162	1.6-214	0.53-1.77	104-36110
Kib	2.6-470	9.75-75.9	0.99-39.5	0.5-147	2.0-2.47	124-4810
Pan	2.6-19.2	1.4-24	0.04-3.1	54-129	<0.1-0.76	337-890
	Na	**Br**	**δ²H**	**δ¹⁸O**	**F**	
Gen	12.4-10113	<0.02-17.3	-100.5-39.8	-0.8-5.47	0.12-13.8	
Öxa	427-10113	2.2-12.1	-100.5-7.1	-12--0.8	0.12-0.7	
Kib	12.4.2163	0.13-17.3	-3.9-39.8	-1.01-5.47	5.12-7.2	
Pan	110-352	<0.02-1.5	-16.6-2.5	-18.8--2.0	2.4-13.8	

4.2 Use of ternary diagram in classifying geothermal waters of Kibiro, Panyimur and Öxarfjördur

4.2.1 Cl-SO₄-HCO₃ ternary diagram

The Cl-SO₄-HCO₃ ternary plot diagram has been used in the classification of geothermal and natural waters (Giggenbach, 1991). Composition of many water types is shown as one of the following in the triangular plot (Figure 4): mature waters, steam-heated waters, volcanic waters and peripheral waters. From the Cl-SO₄-HCO₃ ternary plot, the degree of separation of the plotted points for high-chloride and bicarbonate waters shows some indication of a relative degree of interaction of the fluids at lower temperature with CO₂, and of the HCO₃ contents increasing with time and distance travelled by the waters underground (Giggenbach, 1988).
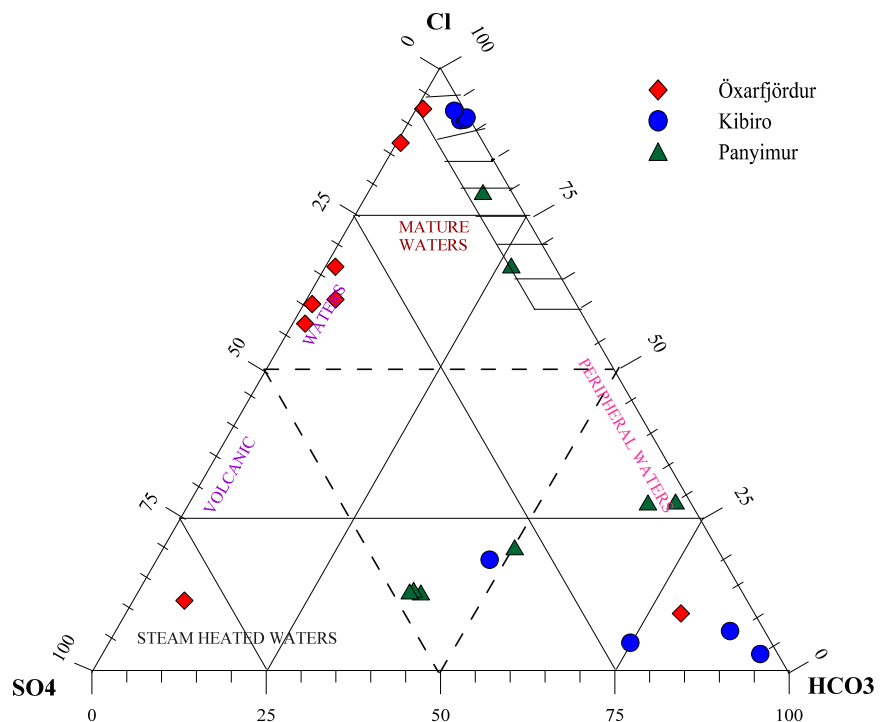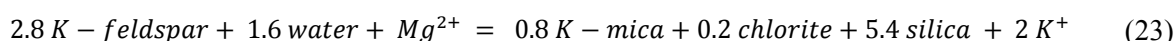

FIGURE 4: Cl-SO₄-HCO₃ ternary plot (Giggenbach, 1991) for water
samples from Kibiro, Panyimur and Öxarfjördur

In Figure 4, for the waters from Kibiro, Panyimur and Öxarfjördur, there is a great degree of variation among the HCO₃ and Cl waters. The waters from the Öxarfjördur area plotted in the volcanic region of the diagram, with two samples in the Cl portions, one in the SO₄ and another one in the HCO₃ part. Four of the Kibiro samples plotted in the chloride portion of the diagram, and three in the HCO₃ region, but

more towards the SO₄ and the HCO₃ section. Two of the Panyimur samples plotted in the Cl area, and two in the peripheral water zone.

4.2.2 The Na-K-Mg triangular diagram

This technique for the derivation of Na-K-Mg-Ca geoindicators was initiated by Giggenbach (1988) as one of the classification techniques for different kinds of water depending on whether they are: 1) immature water; 2) partially equilibrated water; or 3) fully equilibrated water. Using the plots, one may apply geothermometers to the equilibrated and partially equilibrated water only. The triangular diagram, which is temperature dependent, is based on two reactions, Equations 17 and 18.

$$Na - feldspar + K^+ = K - feldspar + Na^+ \qquad (22)$$

$$2.8\,K - feldspar + 1.6\,water + Mg^{2+} = 0.8\,K - mica + 0.2\,chlorite + 5.4\,silica + 2\,K^+ \qquad (23)$$

Equations 22 and 23 are used in the derivation of the geothermometer used.

In the triangular plot, the area of partial equilibrium indicates that there could be some mineral that has dissolved, though it has not yet attained equilibrium or it may be that it is geothermal water, but has been diluted with water that has not yet reached equilibrium, for example cold groundwater. Points which plotted close to the √Mg corner indicate that there is a very high proportion of relatively cold groundwater mixed in the water system.

In Figure 5, 4 samples from Panyimur and 6 samples from Öxarfjördur plotted close to the full equilibrium line but 4 samples from Panyimur and 1 sample from Öxarfjörður plotted in the partially equilibrated region of the diagram, probably meaning that there may be some recharge from cold groundwater into the geothermal systems in those areas. In Kibiro, two of the samples plotted in the immature region, hence contain cold groundwater, while six of the samples plotted in the partially equilibrated portion. The t_{km} temperature for samples from Kibiro varied, ranging between 160°C to 140°C, and then 100°C to <100°C; the tkn was from 100°C to 240°C; for Panyimur, the t_{km} ranged from 120°C to 70°C and the t_{kn} from 100°C to 160°C; for Öxarfjördur, t_{km} varied in the range of <100°C to 200°C and the t_{kn} from 100°C to 200°C. The t_{km} temperature for all these samples varied considerably. This could be due to the fact that the K-Mg geothermometer tends to react faster to change than the K-Na geothermometer in the same system.
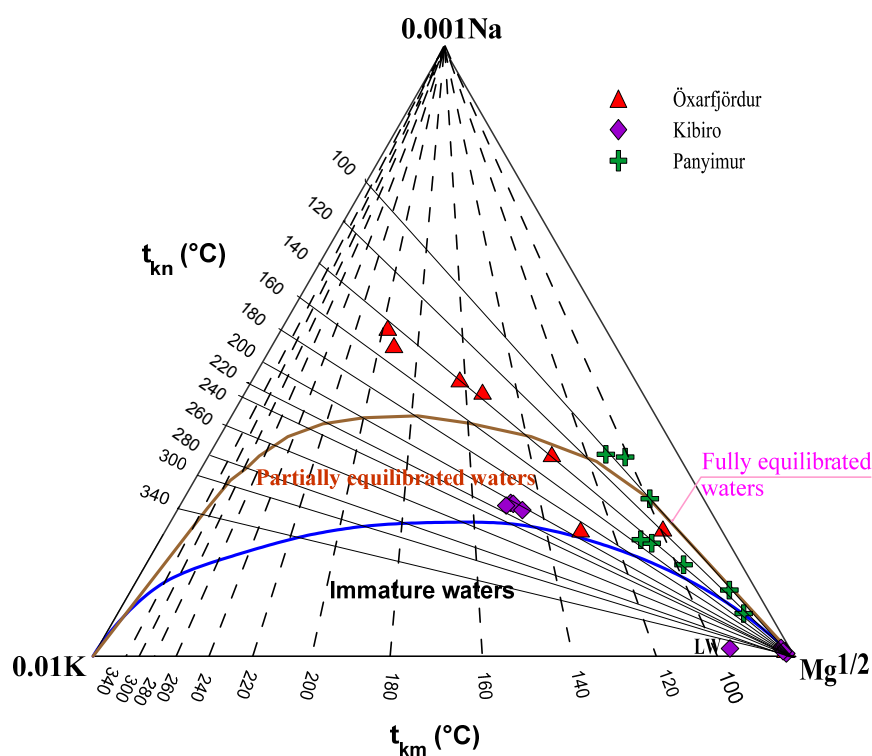

FIGURE 5: Na-K-Mg triangular diagram for samples from Kibiro, Panyimur and Öxarfjördur

4.3 Geothermometer data output

Sixteen different geothermometer Equations (eight for quartz geothermometers, two for chalcedony, three each for Na/K, K-Mg and Na-K-Mg) were applied in the prediction of the subsurface temperatures of the geothermal water from Kibiro, Panyimur and Öxarfjördur. The calculated geothermometer temperatures for eleven geothermometers out of the sixteen are presented in Table 6. The average calculated quartz geothermometer temperature for hot springs and wells in Öxarfjördur was 150°C, in Kibiro samples it was 123°C and in Panyimur it was 129°C. The Na-K geothermometer temperatures for Kibiro and Panyimur were high while the Na-K-Ca geothermometer gave very high temperatures for Öxarfjördur. This may due to loss of CO_2 leading to calcite precipitating out of the solution. This affects the concentration of calcium in the solution, leading to abnormally high geothermometer temperatures. The calculated chalcedony geothermometer temperatures for these samples were: for Öxarfjördur 116°C, for Kibiro 114°C, and for Panyimur 101°C. The calculated Na-K geothermometer temperatures were: for Öxarfjördur 148°C, for Kibiro 197°C and for Panyimur 116°C. Appendix II shows comparison plots of calculated temperature results obtained from sixteen different equations of geothermometers for Öxarfjördur, Kibiro and Panyimur.

TABLE 6: Calculated values for 11 equations for solute geothermometers temperatures (in °C)
for samples from Öxarfjördur, Kibiro and Panyimur

	T_{Na-K}	$T_{Na-K\,1}$	T_{K-Mg}	$T_{qz,\,1}$	$T_{qz,\,2}$	$T_{qz,\,3}$	$T_{qz,\,4}$	$T_{ch\,1}$	$T_{ch\,2}$	$T_{qz,\,5}$	$T_{qz,\,6}$
LOC											
ISK	139.6	129.77	132.6	152	153.80	150.2	143.08	136.42	132.7	160.33	160.39
ISG	144.4	134.79	197.4	142.6	144.1	137.82	132.77	123.60	121	148.95	148.94
IBK	191.1	183.73	130	132.9	134.1	125.35	122.23	110.68	109.2	137.36	137.39
IA1	150.3	140.89	191.9	148.8	150.5	145.97	139.57	132.03	128.7	156.46	156.48
IA3	136.9	127.01	153.1	145.1	146.7	141.10	135.5	126.99	124.1	151.98	151.98
IA4	140.8	131.01	161.5	171.9	174.2	176.99	165.12	164.22	157.9	185.61	185.08
IJÖ	162.1	153.24	35.97	63.23	56.68	41.81	43.03	24.71	28.64	57.01	57.12
ISW	115.6	104.91	98.38	1.29	-35.28	-39.53	-48.75	-43.10	-36.85	-10.61	-27.54
KIB											
KM1	205.36	198.79	148.7	145.1	146.7	141.05	135.47	126.94	124.1	151.93	151.93
KM2	204.98	198.39	148.00	143.5	145.1	139.01	133.76	124.83	122.1	150.05	150.04
KM3	206.4	199.84	145.7	142.3	143.8	137.45	132.46	123.22	120.7	148.61	148.60
KM4	210.6	204.31	150.1	147.3	149.00	144.03	137.95	130.03	126.90	154.67	154.69
KM4	182.30	174.43	45.87	131.7	131.9	131.85	131.85	128.08	103.4	104.41	131.77
KM6	285.1	284.34	40.18	118.8	119.00	119.00	119.00	117.11	90.25	90.24	119.05
KM7	238.90	234.54	45.34	122.5	122.7	122.69	122.69	120.27	94.02	94.29	122.70
KM8	532.3	564.09	92.86	-34.8	65.25	65.25	65.25	-21.62	-59.76	-66.38	-67.87
PAN											
PA1	99.73	88.62	110.9	118.4	119.1	107.31	106.58	91.94	91.84	120.34	120.59
PA2	96.83	85.64	98.15	116	116.5	104.30	103.90	88.81	88.93	117.46	117.77
PA3	137.9	128.06	72.33	105.7	105.5	91.79	92.57	75.78	76.80	105.44	105.97
PA4	83.04	71.54	101.5	116.6	117.2	105.06	104.58	89.6	89.67	118.19	118.48
PA5	108.1	97.21	74.13	115.4	115.9	103.53	103.21	88.01	88.18	116.72	117.04
PA6	141	131.22	96.34	140.7	142.2	135.34	130.68	121.03	118.7	146.66	146.64
PA7	147.3	137.81	106.7	145.1	146.7	141.05	135.47	126.94	124.1	151.93	151.93
PA8	153.9	144.70	110.6	145.1	146.7	141.05	135.47	126.94	124.1	151.93	151.93

Note:　　T_{Na-K}=Na-K cation geothermometer;　　　T_{K-Mg}=K-Mg cation geothermometer;
　　　　$T_{qz\,(1-6)}$ =Quartz geothermometers;　　　　$T_{ch\,(1\,and\,2)}$=Chalcedony geothermometer.

In many instances there was not a good agreement between the Na-K temperatures and the silica temperatures for samples from Öxarfjördur, but the cation geothermometers seemed to agree quite closely. The quartz geothermometer temperatures for Kibiro seemed to agree quite well, and for the Panyimur samples, there were great variations in all the calculated geothermometer temperatures. The magnesium concentrations were high in these samples, suggesting a substantial influence of cold

groundwater, rendering the Na/K geothermometer unreliable; at low temperatures, the silica geothermometers are not dependable either.

The anomalously high estimates from the Na-K-Ca geothermometer for all the samples could be due to calcium carbonate deposited during the ascent which prevents aqueous K and Na from interacting with the country rock (Fournier and Truesdell, 1973).

Geothermometers take advantage of specific mineral –solute reactions (Karingithi, 2009) which are slow to equilibrate at cooler temperatures, especially under conditions where the fluid is effectively separated from the minerals which control the equilibria. The result is that a hot equilibrium temperature is "frozen in" to the fluid, reflected by solute concentrations or solute ratios.

4.4 Mixing model interpretations

Assuming that the silica has not precipitated before or after mixing and that there has been no conductive cooling of the water, then the dissolved silica concentration of a mixed water and a silica – enthalpy diagram may be used to determine the temperature of the hot water component. However, it is not easy to determine whether a given spring is a mixture of hot and cold spring water and also to prove that silica has not precipitated or that conductive cooling has not occurred (Truesdell and Fournier, 1977).

From the enthalpy – silica mixing model (Figure 6), the samples from Kibiro indicate a geothermal system with a temperature of about 191-220°C; samples from Panyimur indicate temperatures of about 150-160°C, and samples from Öxarfjördur show temperatures of 190-220°C.
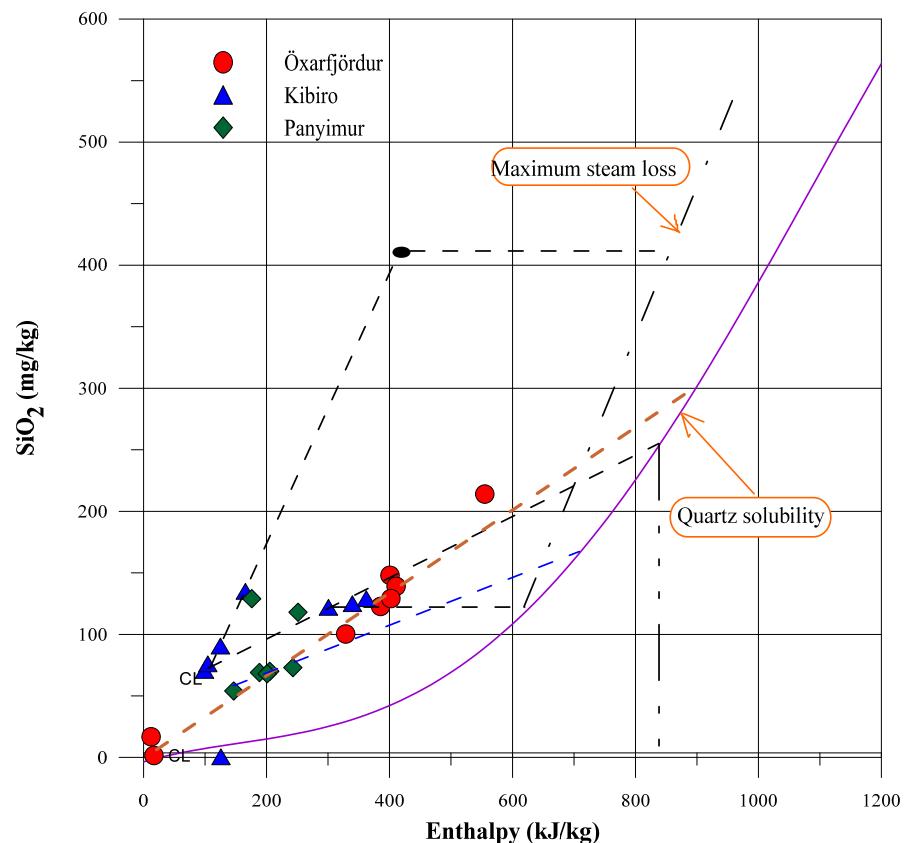
FIGURE 6: Silica-enthalpy mixing model applied to water samples from Kibiro, Panyimur and Öxarfjördur

The silica – carbonate plot (Figure 7) for all the samples from Panyimur indicates that boiling has not occurred; for Kibiro, two of the samples showed boiling in the hot spring while some showed equilibration and others suggested no boiling or mixing. Samples from Öxarfjördur suggested that boiling had occurred, meaning that some of the CO_2 had been lost in the steam phase, hence lowering the CO_2 concentrations in some of those samples.

4.5 Gas geothermometer temperature results based on this analysis

Gas geothermometer temperatures were calculated for one sample from Kibiro and the results were: T_{CO2} =199°C, $T_{CH4/C2H6}$ = 208°C and $T_{H2/Ar}$ = 221°C. For the samples from Öxarfjördur, the following estimates of $T_{CH4/C2H6}$ were made on three well samples; these showed the following temperature ranges: Well AER-01 = 150-170°C; Well AER-03 = 175-180°C; and Well AER-04 = 200-220°C. This was done basically to confirm the variations of gas geothermometers and the chemical or solute geothermometers.
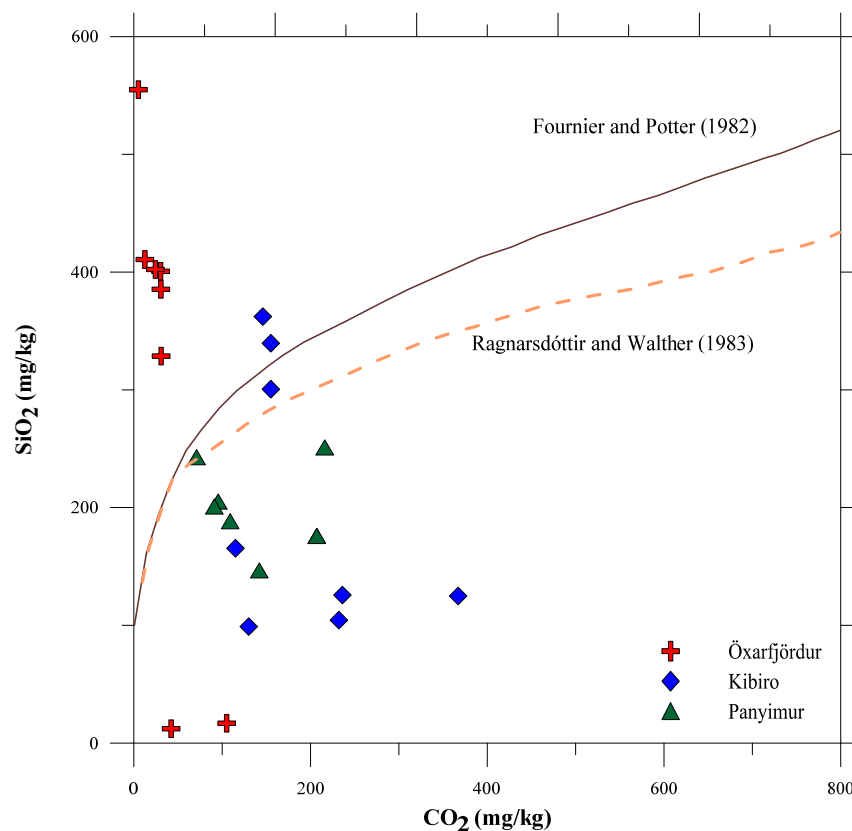
FIGURE 7: Silica versus carbon dioxide

4.6 Binary plots

A mixing trend can be clearly seen in all the areas under study as shown in Figure 8a, K^+ vs. Cl^- and in Figure 8b, Na^+ vs. Cl^-, with positive correlations for Öxarfjördur and Kibiro, which may mean that there is a high Cl^- concentration possibly being added into these systems. In Öxarfjördur, it could be that seawater is mixing with the geothermal waters. In Kibiro, the source may be from the salt mining in that area and/or sodium chloride geothermal waters. For Panyimur, sodium chloride geothermal waters may be mixing at depth.

The concentration of HCO_3, shown in Figure 8c, in four samples from Kibiro and in two samples from Panyimur is relatively higher than in other samples, suggesting that there could be CO_2 absorption from the gases that the fluid carries or from the condensation of geothermal steam containing CO_2 in the particular geothermal water samples containing high concentrations of HCO_3. There is an increase in the concentration of chloride in the samples from Öxarfjördur which may mean that there is either mixing of the geothermal waters with sea water or with deep geothermal fluids.

Looking at the relationships of different elements in the geothermal waters from Kibiro, Panyimur and Öxarfjördur (Figure 9), the following conclusions may be drawn from these results. There are some linear relationships between B and Cl (Figure 9a) which may mean that there is mixing of cold water with hot geothermal fluid in the upflow zones in these systems. For the Kibiro samples, there seems to be a linear relationship between Li and Cl (Figure 9b) that may be due to the uptake of lithium from the waters by the surrounding rocks in the area, suggesting that there could be some water rock interaction in the system

The relationships between Na – B and Ca – B (Figures 9c and d) in which B is a conservative element, and a linear relationship in the plots of these samples may mean that Ca and Na are present in the environment in which these waters occur; the increase in the B concentration suggests that there is water-
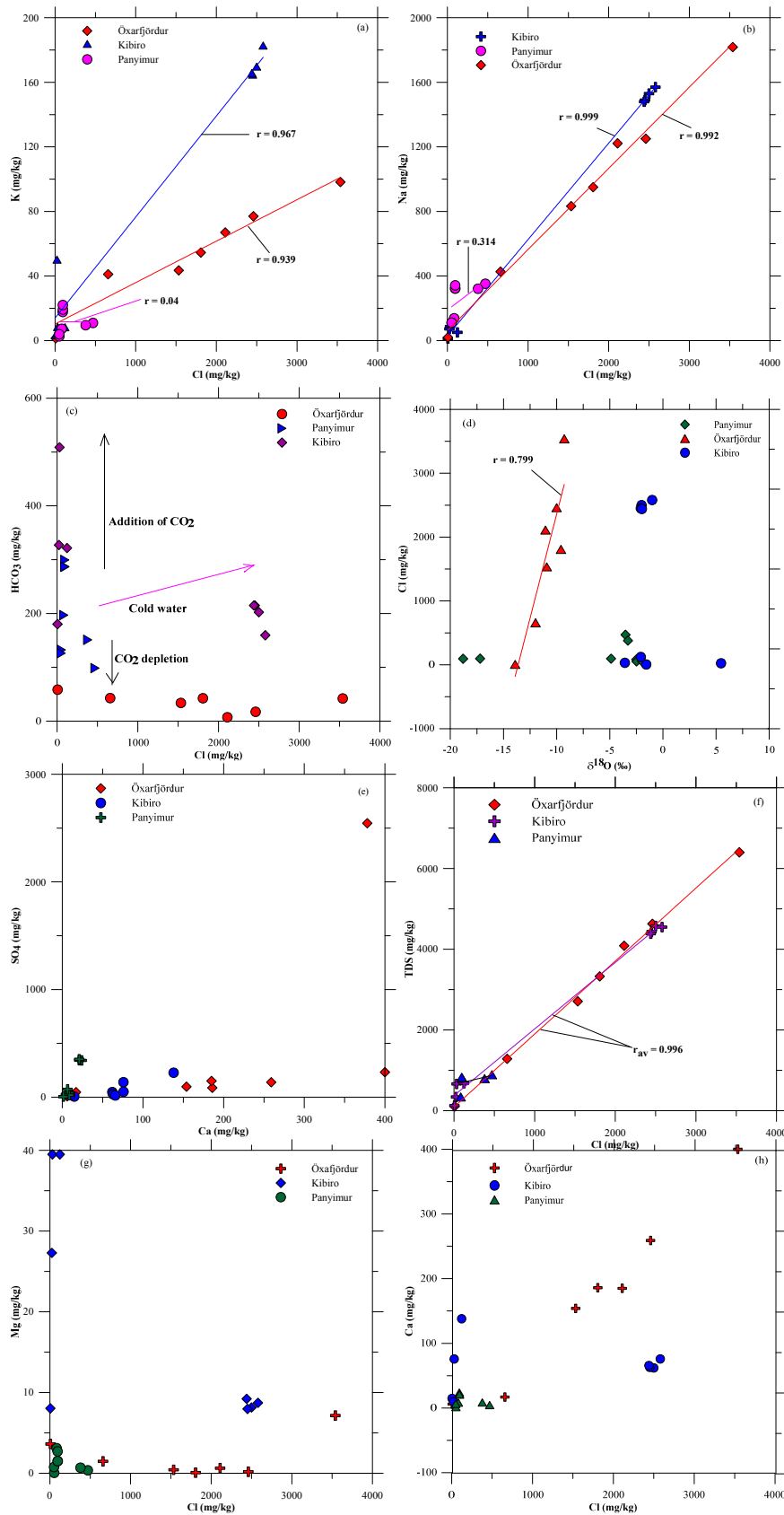
FIGURE 8: Binary plots of K vs. Cl, Na vs. Cl, HCO3 vs. Cl, Cl vs.
$\delta^{18}O$, SO4 vs. Ca, TDS vs. Cl, Mg vs. Cl, and Ca vs. Cl

rock interaction since Ca and Na are less mobile compared to B, and may be removed from the water during secondary mineral precipitation out of the solution.

Clear linear relationships are observed for $\delta^{18}O$ and Cl in samples from Öxarfjörður (Figure 8d) which may be due to mixing of saline and non-saline component and/or water-rock interaction and B and Cl in samples from all three areas (Figure 9a) suggesting water-rock interaction.
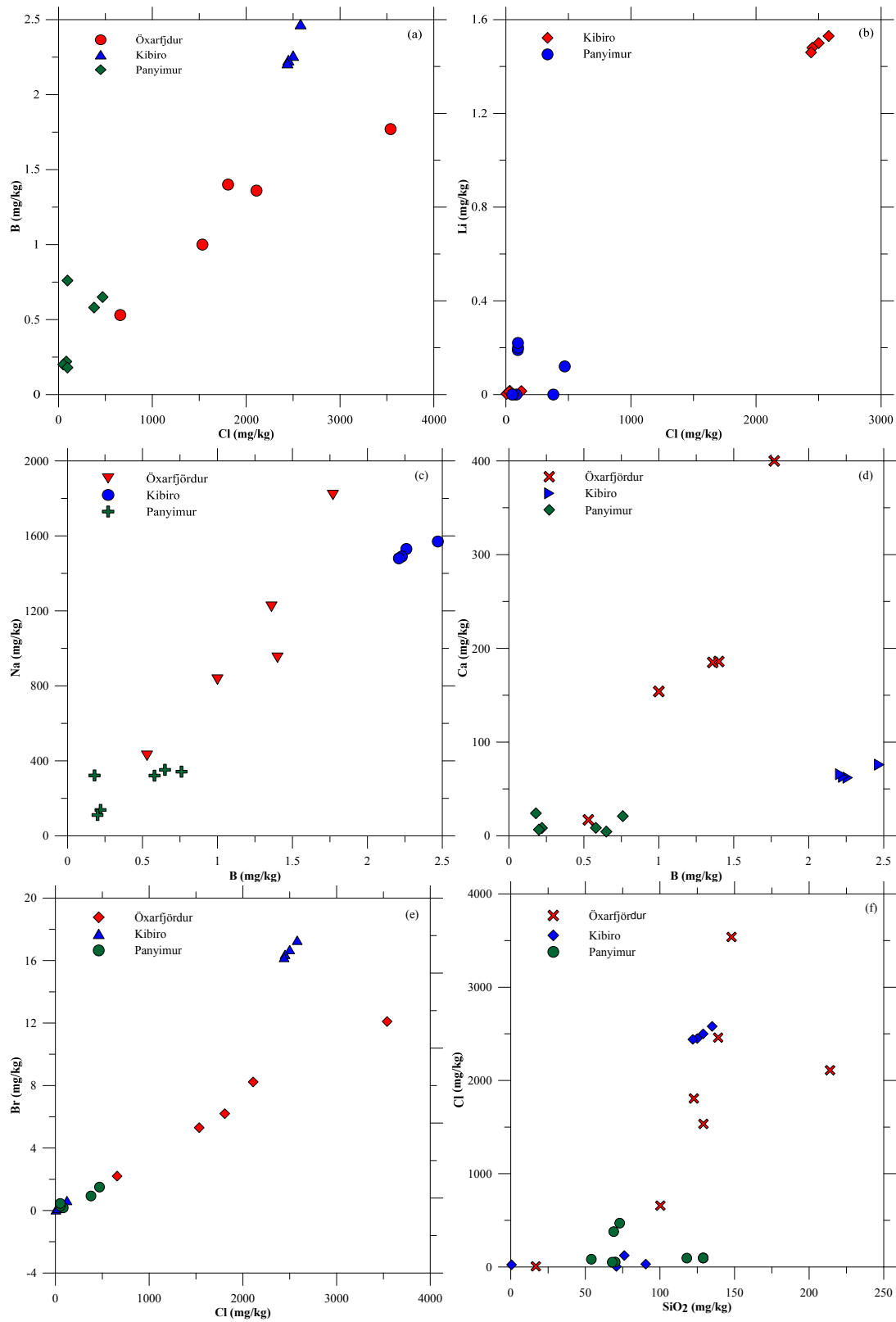
FIGURE 9: Binary plots of B vs. Cl, Li vs. Cl, Na vs. B,
Ca vs. B, B vs. Cl and Cl vs. SiO₂

4.7 Mineral saturation

In the log (Q/K) plots showing the equilibrium state of some of the minerals calculated by the WATCH programme for Kibiro samples (Figure 10), most of the curves intersect the line of log (Q/K) equal to zero for Kibiro area in the temperature range 140 – 160°C, and some of the minerals converge below the log (Q/K) equal to zero line at 180 ->200°C. For Panyimur, most of the curves cross the log (Q/K) equal to zero line at 120 – 160°C and converge below it at 180 – > 200°C. For Kibiro and Panyimur, it may be inferred that there is some mixing of cold water with a geothermal component. The anhydrite in the samples from Kibiro and Panyimur are undersaturated. Samples from Öxarfjördur (Figure 11) show that most of the minerals have not yet reached equilibrium. The curves for the different minerals intersect the log (Q/K) line equal to zero at temperatures of about 120 – 150°C. And some of the curves converge below the log (Q/K) line equal to zero at temperatures of about 90 – 180°C, with some curves converging above 200°C. There is some mixing of cold water with a geothermal component in the Öxarfjördur area. And most of the minerals are undersaturated, that is their solubility, for example, of hydrate, talc, and calcite decreases (Stefánsson et al., 2000) with increasing temperature leading to their being precipitated out of the solution. This may be due to mixing of hot water with cold water in the area.

4.7.1 More output from the WATCH programme

The WATCH speciation program (Bjarnason, 2010; Arnórsson et al., 1983a) was used in the calculation of the mineral equilibria, based on the fact that different minerals have different reaction quotients and equilibrium constants. The ionic balance values for two samples from Öxarfjördur, four samples from Kibiro and two samples from Panyimur are above 5%, but the rest are below 5%.

4.8 Isotope data interpretation

In the Öxarfjördur area, the $\delta^{18}O$ ranges from -12.0 to -0.8 ‰ and δ^2H from -100.4 to -7.1 ‰; in Kibiro: $\delta^{18}O$ from 5.5 to -1.0 ‰ and δ^2H from +39.8 to - -3.9 ‰, and for Panyimur: $\delta^{18}O$ values range from -18.8 to -2.0 ‰, then δ^2H from 2.5 to -16.6 ‰. There is a significant variation in the $\delta^{18}O$ values of these three areas**.**

All Kibiro samples plotted close to: the WML, KRL and CARL lines, with some slight shift from the WML line (Figure 12) which may mean that there is some oxygen shift due to water rock interaction within the system as a result of a low water rock ratio or a high temperature. All samples from Panyimur plotted above the lines, suggesting that there could be some good permeability in the area; this could also mean that there is excess deuterium.

The samples from Öxarfjördur all plotted below the KRL and CARL lines, but close to the WML line. This could mean that the water samples from Öxarfjördur have undergone water rock interaction for a relatively long time and there may be a high temperature at depth, hence leading to oxygen shift due to the exchange of oxygen between water and the rock.
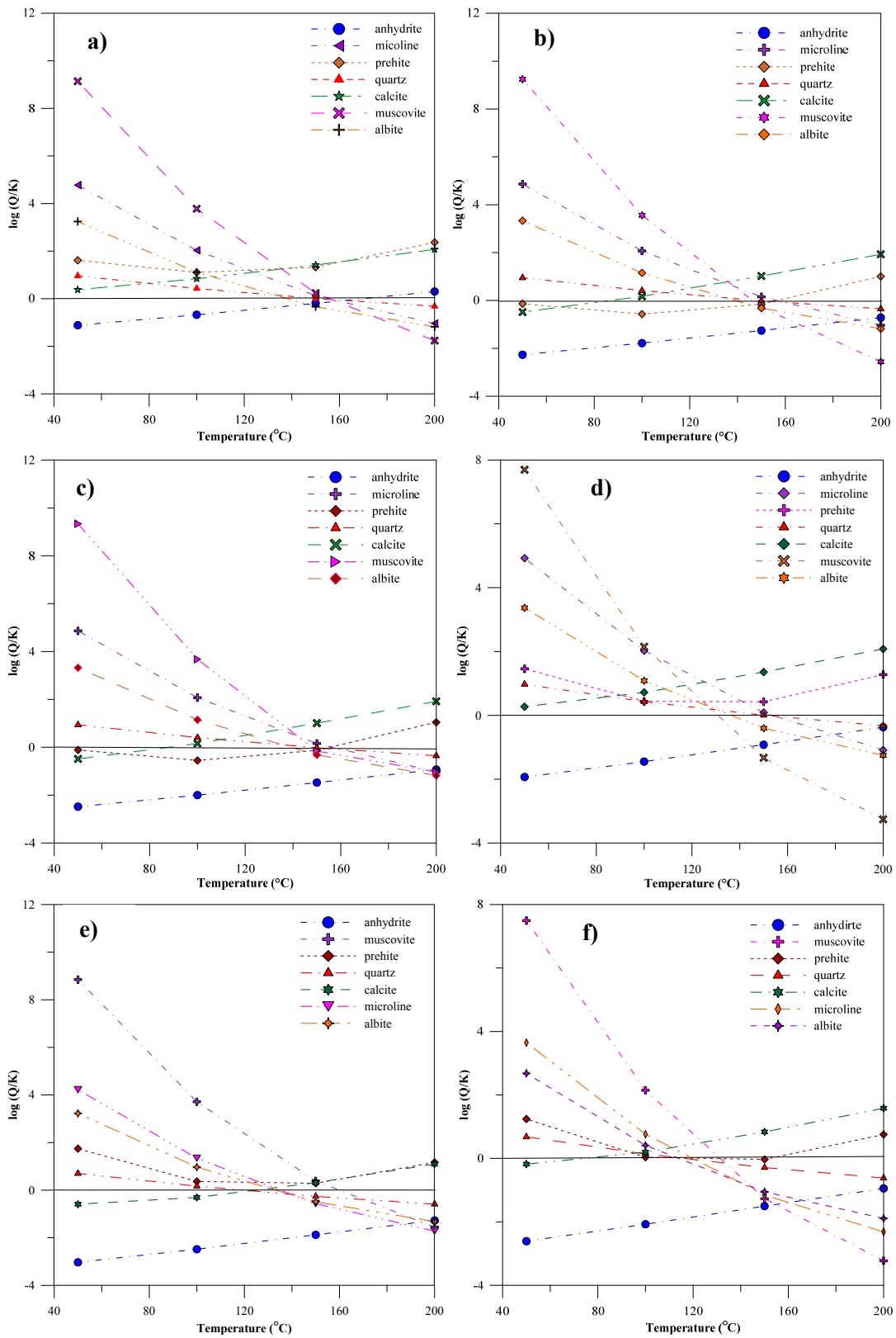
FIGURE 10: Mineral equilibrium plots for Kibiro samples
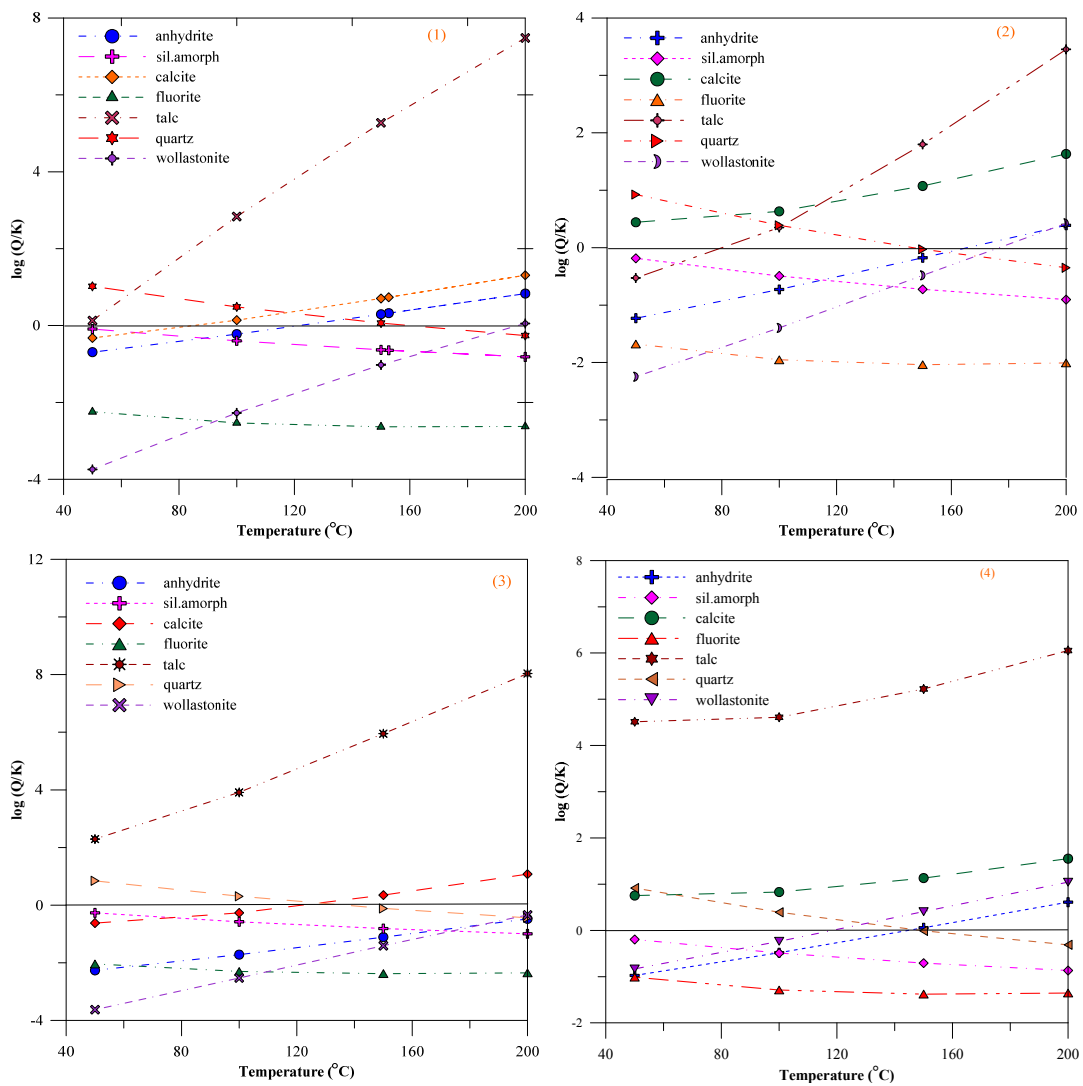(a – d) and Panyimur samples (e and f)

FIGURE 11: Mineral equilibrium plots for Öxarfjördur

5. CONCLUSIONS

- The geothermal waters of Kibiro, Panyimur and Öxarfjördur are classified as sodium-chloride-bicarbonate waters. The geothermal samples from Öxarfjördur are more mature than the water samples from Kibiro and Panyimur.

- From geothermometer temperature prediction and interpretation, quartz and Na/K geothermometers are applicable in a very wide range of geological environments, for example from rhyolitic, classic sediments to a basaltic geological setting.

- The mineral saturation plots for Kibiro and Panyimur showed that all waters had almost reached equilibration with most minerals, but in Öxarfjördur they have not yet attained equilibrium.

- The chemical composition of the water samples from Kibiro, Panyimur and Öxarfjördur, with different sedimentary geological settings, is much affected by the strata through which these fluids flow.

- Despite the fact that the Öxarfjördur geothermal system is located in a sedimentary graben, there is considerable water- rock interaction at depth beneath the sedimentary system compared to the situation at Kibiro and Panyimur.

FIGURE 12: Plot of δ^2H vs $\delta^{18}O$ for samples from Kibiro, Panyimur and Öxarfjördur

5.1 Recommendations and future research work

- More geochemical exploration work needs to be carried out in geothermal systems occurring in sedimentary geological settings for better interpretation of the geochemistry of these systems.

- Combined geochemical, geological and geophysical studies are required for better understanding of geothermal systems in sedimentary settings.

- A distribution map for deuterium ratios and full geological maps of the geothermal systems in Kibiro and Panyimur are required.

- The geochemistry of the hot spring discharges in Kibiro and Panyimur may be controlled by the interaction of the fluids with the crystalline basement, and is characterized by low B/Cl conservative element ratios and a high pH. This needs more research.

- From this study, the application of geothermometry techniques clearly differ from one place to another due to the different environmental conditions, such as physical processes like conductive cooling and mixing with cold water. Boiling during upflow may affect possible water-rock equilibria in the deep reservoir, and this can result in unreliable temperature predictions. Furthermore, it is very useful to employ different geothermometers and methods for studying equilibrium states in order to check each and to exclude unreliable samples and non-applicable geothermometers.

NOMENCLATURE

EARS = East Africa Rift System
ISOR = Iceland GeoSurvey
MEMD = Ministry of Energy and Mineral Development
CARL = Continental African rain line
WML = World meteoric line
KRL = Kenyan rain line
GSMD = Geological Survey and Mines Department
UNU = United Nations University
TDS = Total dissolved solids
OS = Orkustofnun
ICEIDA = Icelandic International Development Agency
IAEA = International Atomic Energy Agency
LOC = Location
KIB = Kibiro
ÖXA = Öxarfjördur
PAN = Panyimur

AAS = Atomic absorption spectrophotometry
IC = Ion chromatography
ISE = Ion specific electrode
FAAS = Flameless atomic absorption spectrophotometry
GC = Gas chromatography
USI = University of Iceland science institute, Reykjavik
n.c. = non-condensable
MS = Mass spectrometry
T = Temperature in (^{o}C)
Tqz (1-8)   = Temperature obtained using quartz geothermometer
Tch (1-2)   = Temperature obtained using chalcedony geothermometer
TK-Mg, TNa-K, TNa-K and Na-K-Ca are different cation geothermometers used to obtain
   the temperature

REFERENCES

Afeworki O., M., 2010: Analysis of temperature and pressure characteristics of the Hverahlíd geothermal field in the Hengill geothermal system, SW-Iceland. Report 20 in: *Geothermal training in Iceland 2010*. UNU-GTP, Iceland, 1-28.

Ármannsson, H., 2009: Application of geochemical methods in geothermal exploration. *Proceedings of the "Short Course IV on Exploration for Geothermal Resources" organized by UNU-GPT, KenGen and GDC, at Lake Naivasha, Kenya,* 8 pp.

Ármannsson, H., 2010*: Investigations of geothermal areas in Uganda other than Katwe-Kikorongo, Buranga and Kibiro*. ÍSOR – Iceland GeoSurvey, prepared for ICEIDA, report ÍSOR-2010/003, 1-17 pp.

Ármannsson, H., 2013: *Fluid chemistry and utilization.* UNU-GTP, Iceland, unpublished lecture notes, 22 pp.

Ármannsson, H. and Ólafsson, M., 2006: *Collection of geothermal fluids for chemical analysis*. ÍSOR – Iceland GeoSurvey, Reykjavík, report ISOR-2006/016, 17 pp.

Árnason, K., and Gíslason, G., 2009: Geothermal surface exploration. *Paper presented at "Short Course on Surface Exploration for Geothermal Resources", organized by UNU-GTP and LaGeo, Santa Tecla, El Salvador,* 7 pp.

Arnórsson, S. (ed.), 2000a: Isotopic and chemical techniques in geothermal exploration, development and use. *Sampling methods, data handling, and interpretation. International Atomic Energy Agency, Vienna,* 351 pp.

Arnórsson, S., 2000b: The quartz and Na/K geothermometers. I. New thermodynamic calibration. *Proceedings of the World Geothermal Congress 2000, Kyushu-Tohoku, Japan,* 929-934.

Arnórsson, S., and Bjarnason, J.Ö., 2007: Fluid-fluid interaction in geothermal systems. *Reviews in Mineralogy & Geochemistry, 65,* 229-312.

Arnórsson, S., and Svavarsson, H., 1985: Application of chemical geothermometry to geothermal exploration and development. *Geoth. Res. Council, Transactions, 9-1,* 293-298.

Arnórsson, S. (ed.), D'Amore, F., and Gerardo-Abaya, J., 2000*: Isotopic and geochemical techniques in geothermal exploration, development and use: Sampling methods, data handling, and interpretation.* International Atomic Energy Agency, Vienna, 351 pp.

Arnórsson, S., Gunnarsson, I., Stefánsson, A., Andrésdóttir, A., and Sveinbjörnsdóttir, Á.E., 2002: Major element chemistry of surface- and ground waters in basaltic terrain, N-Iceland. I. Primary mineral saturation. *Geochim. Cosmochim. Acta, 66,* 4015-4046.

Arnórsson, S., Gunnlaugsson, E., and Svavarsson, H., 1983: The chemistry of geothermal waters in Iceland. III. Chemical geothermometry in geothermal investigations. *Geochim. Cosmochim. Acta, 47,* 567-577.

Atekwana, E.A., Hogan, J.P., Kampunzu, A.B., and Modisi, M.P., 2004: Early structural evolution of the nascent Okavango rift zone, NW Botswana. *Proceedings of the East African Rift System: Geodynamics, Resources, and Environment Conference, Addis Ababa,* 12-16.

Bahati, G., 2007: Status of geothermal energy exploration in Uganda. *Paper presented at "Short course II on surface exploration for geothermal resources, Naivasha Kenya", organized by UNU-GTP, Iceland, and KenGen, Naivasha, Kenya,* CD SC-05, 10 pp.

Bahati, G., 2012: Status of geothermal exploration and development in Uganda. *Paper presented at "Short Course VII on Exploration for Geothermal Resources, organized by UNU-GTP, GDC and KenGen, at Lake Bogoria and Lake Naivasha, Kenya,* 14 pp.

Bertrami, R., Cioni, R., Corazza, E., D´Amore, F., and Marini, L., 1985: Carbon dioxide in geothermal gases. Reservoir temperature calculations at Larderello (Italy). *Geothermal Research Council, Transactions, 9,* 299-303.

Bjarnason, J.Ö., 2010: *The speciation program WATCH, Version 2.4.* The Iceland Water Chemistry Group, Reykjavík.

Björnsson, A., Eysteinsson, H., and Beblo, M., 2005: Crustal formation and magma genesis beneath Iceland: magnetotelluric constraints. In: Foulger, G.R., Natland, J.H., Presnall, D.C., Anderson, D.L. (eds.), *Plates, plumes and paradigms*. Geological Society of America, Spec. Pap. 388,665–686.

Bruhn, D., Manzella, A., Vuataz, F., Faulds, J., Moeck, I., and Erbas, K., 2011: Exploration methods. In: Huenges, E. (ed.), *Geothermal energy systems.* Wiley-VCH Verlag GmbH, Weinheim, 465 pp.

Craig, H., 1963: The isotopic geochemistry of water and carbon in geothermal areas. In: Tongiorgi, E. (ed.), *Nuclear geology on geothermal areas.* Consiglio Nazionale delle Ricerche, Laboratorio di Geologia Nucleare, Pisa, 17-53.

D'Amore, F., and Arnórsson, S., 2000: Geothermometry. In: Arnórsson, S. (ed.), *Isotopic and chemical techniques in geothermal exploration, development and use. Sampling methods, data handling, interpretation.* International Atomic Energy Agency, Vienna, 152-199.

D'Amore, F., Krajca, J., Michard, G., Nuti, S., Ólafsson, M., Paces, T., Zhaoli, S., Wei, T., and Zhifei, Z., 1991: *Fluid sampling for geothermal prospecting.* UNITAR/UNDP Centre on Small Energy Resources, Rome, 93-117 pp.

Data, G., and Bahati, G., 2003: The chemistry of geothermal waters from areas outside the active volcanic belt, SW-Uganda. *Proceedings of the 2nd KenGen Conference, Nairobi, Kenya, April 2003,* 24-29.

Driesner, T, 2013: Geothermal activities in the Main Ethiopian Rift: Hydrogeochemical characterization of geothermal waters and geothermometry applications (Dofan-Fantale, Gergede-Sodere, Aluto-Langano). *Geothermics, 47,* 1-12.

Ebinger, C.J., Deino, A.L., Drake, R.E., and Tesha, A.L., 1989: Chronology of volcanism and rift basin propagation: Rungwe volcanic province, East Africa. *J. Geophys. Res., 94-B11:15*, 785-803.

EDICON, 1984: *Aeromagnetic interpretation of Lake Albert/Edward portion of the Western Rift Valley.* EDICON, Inc., Denver, Colorado, unpublished report.

Ellis, A.J., and Mahon, W.A.J., 1977: *Chemistry and geothermal systems.* Academic Press, New York, 392 pp.

Fournier, R.O., 1977: Chemical geothermometers and mixing model for geothermal systems. *Geothermics, 5,* 41-50.

Fournier, R.O., 1979: A revised equation for Na-K geothermometer. *Geoth. Res. Council, Trans., 3,* 221-224.

Fournier, R.O., and Potter, R.W., 1982: An equation correlating the solubility of quartz in water from 25° to 900°C at pressures up to 10,000 bars. *Geochim. Cosmochim Acta, 46*, 1969-1973.

Fournier, R.O., and Truesdell, A.H., 1973: An empirical Na-K-Ca geothermometer for natural waters. *Geochim. Cosmochim. Acta*, *37*, 1255-1275.

Georgsson, L.S., Árnason, K., and Karlsdóttir, R., 1993: Resistivity sounding in high-temperature areas in Iceland, with examples from Öxarfjördur, N-Iceland and Brennisteinsfjöll, SW-Iceland. *Proceedings of the 14th PNOC-EDC Geothermal Conference, Manila*, 9 pp.

Georgsson, L.S., Fridleifsson, G.Ó., Ólafsson, M., and Flóvenz, Ó.G., 2000: The geothermal exploration of the Öxarfjördur high-temperature area, NE-Iceland. *Proceedings of the World Geothermal Congress 2000, Kyushu-Tohoku, Japan,* 1157-1162.

Giggenbach, W.F., 1980: Geothermal gas equilibria. *Geochim. Cosmochim. Acta, 48*, 2693-2711.

Giggenbach, W.F., 1984: Mass transfer in hydrothermal alteration systems – A conceptual approach. *Geochim. Cosmochim. Acta, 48*, 2693–2711.

Giggenbach, W.F., 1988: Geothermal solute equilibria. Derivation of Na-K-Mg-Ca geoindicators. *Geochim. Cosmochim. Acta, 52*, 2749-2765.

Giggenbach, W.F., 1991: Chemical techniques in geothermal exploration. In: D'Amore, F. (coordinator), *Application of geochemistry in geothermal reservoir development.* UNITAR/UNDP publication, Rome, 119-144.

Giggenbach, W.F., 1992: Isotope shift in waters from geothermal and volcanic systems along convergent plate boundaries and their origin. *Earth and Planetary Sci. Lett., 113*, 495-510.

Giggenbach, W.F., Sheppard, D.S., Robinson, B.W., Stewart, M.K., and Lyon, G.M., 1994: Geochemical structure and position of the Waiotapu geothermal field, New Zealand. *Geothermics, 23,* 599-644.

Gíslason, G., Ngobi, G., Isabirye, E., and Tumwebaze, S. 1994: *An Inventory of three Geothermal Areas in West and Southwest Uganda.* Prepared by the United Nations for a Project of the UNDP.

Gíslason, G., Ívarsson, G., Gunnlaugsson, E., Hjartarson, A., Björnsson, G., and Steingrímsson, B., 2005: Production monitoring as a tool for field development; A case history from the Nesjavellir field, Iceland. *Proceedings of the World Geothermal Congress 2005, Antalya, Turkey,* 9 pp.

GSMD, 2008: *Exploration report by the geological team of DGSM.* DGSM, Entebbe, unpublished report.

Henley, R.W. and Ellis, A.J. 1983: Geothermal systems ancient and modern: a geochemical review. *Earth Science and Reviews, 19,* 1-50.

Henley, R.W., Truesdell, A.H., and Barton, P.B. Jr., 1984: *Fluid-mineral equilibrium in hydrothermal systems.* Society of Economic Geologists, Reviews in Economic Geology, 1, 267 pp.

Hjartarson, A., Axelsson, G., and Xu Y., 2005: Production potential assessment of the low-temperature sedimentary geothermal reservoir in Lishuiqiao, Beijing, P.R. of China, based on a numerical simulation study. *Proceedings of the World Geothermal Congress 2005, Antalya, Turkey,* 12 pp.

Jónsson, G., Kristjánsson, L., and Sverrisson M., 1991: Magnetic surveys of Iceland. *Tectonophysics 189*, 229-247.

Kato, V., 2003: *Chemistry of thermal springs in Uganda.* Geological Survey and Mines Department, Entebbe, report KVK/14, 2 pp.

Karingithi, C.W., 2009: Chemical geothermometers for geothermal exploration, *Paper presented at Short Course IV on Exploration for Geothermal Resources, organized by UNU-GTP, KenGen and GDC, at Lake Naivasha, Kenya*, 12 pp.

Marini, L., and Cioni, R., 1985: A chloride method for the determination of the enthalpy of steam/water mixtures discharged from geothermal wells. *Geothermics, 14*, 29-34.

Mosley, P.N., 1993. Geological evolution of the late Proterozoic "Mozambique belt" of Kenya. *Tectonophysics, 221,* 223-250.

Natukunda.J.F., 2013: *Exploration report on the follow up of the geology of Panyimur by the geological team of DGSM.*DGSM, Entebbe, unpublished report.

Noda, T., and Shimada K., 1993: Water mixing model calculation for evaluation of deep geothermal water. *Geothermics, 22*, 165-180.

Ólafsson, M., Fridleifsson, G.Ó., Eiríksson, J., Sigvaldasson, H., and Ármannsson, H., 1993: *On the origin of organic gas in Öxarfjördur, NE-Iceland*. Orkustofnun, Iceland, report OS-93015/JHD-05, 76 pp.

Reed, M.H., 1991: Computer modelling of chemical processes in geothermal systems: Examples of boiling, mixing and water-rock reaction. In: D´Amore, F. (coordinator), *Applications of geochemistry in geothermal reservoir development.* UNITAR/UNDP publication, Rome, 275-297.

Rodríguez, A., 2011: *Water-rock interaction of silicic rocks: an experimental and geochemical modelling study.* University of Iceland, MSc thesis, UNU-GTP, Iceland, report 1, 44 pp.

Rybach, L., and Muffler, L.J.P. (eds.), 1981: *Geothermal systems, principles and case histories.* John Wiley & Sons, Ltd., Chichester, 359 pp.

Stefánsson, A., Gíslason, S.R., and Arnórsson, S., 2000: Dissolution of primary minerals in natural waters II. Mineral saturation state. *Chemical Geology, 172,* 251-276.

Stefánsson, A., Gunnarsson, I., and Giroud, N., 2007: New methods for the direct determination of dissolved inorganic, organic and total carbon in natural waters by Reagent-Free™ IonChromatography and inductively coupled plasma atomic emission spectrometry. *Analytical ChimicaActa, 582*, 69-72.

Truesdell, A.H., 1991: Origin of acid fluids in geothermal reservoirs. *Geotherm. Res. Counc.,Trans., 15*, 289-296.

Truesdell, A.H., and Fournier, R.O., 1976: Calculations of deep temperatures in geothermal systems from the chemistry of boiling spring waters of mixed origin. *Proceedings of 2nd U.N. Symposium on the Development and Use of Geothermal Resources, San Francisco, 1,837-844.*

Truesdell, A.H., and Fournier, R.O., 1977: Procedure for estimating the temperature of a hot water component in a mixed water using a plot of dissolved silica vs. enthalpy. *U.S. Geol. Survey J. Res., 5,* 49-52.

Verma, S.P., and Santayo, E., 1997: New improved equations for Na/K, Na/Li and SiO_2 geothermometers by outlier detection and rejection. *J. Volcanol. Geotherm. Res., 79*, 9-23.

Wood, J., and Guth, A., 2012: *East Africa's Great Rift Valley, a complex rift system.* Geology.com, webpage: *geology.com/articles/east-africa-rift.shtml.*

Yohannes B., E. 2004: Geochemical interpretation of thermal water and gas samples from Krýsuvík, Iceland and Alid, Eritrea. Report 18 in: *Geothermal training in Iceland 2004*. UNU-GTP, Iceland, 403-438.

APPENDIX I: Maps of Kibiro and Panyimur (source DGSM, 2013)
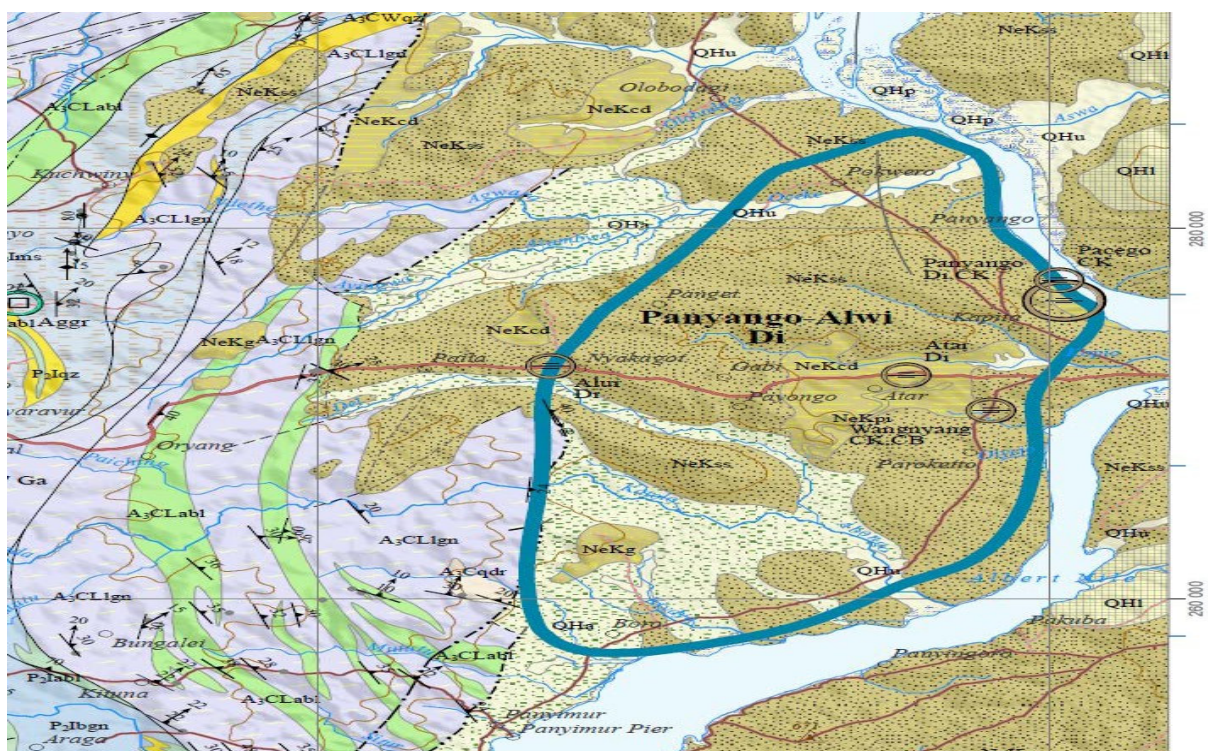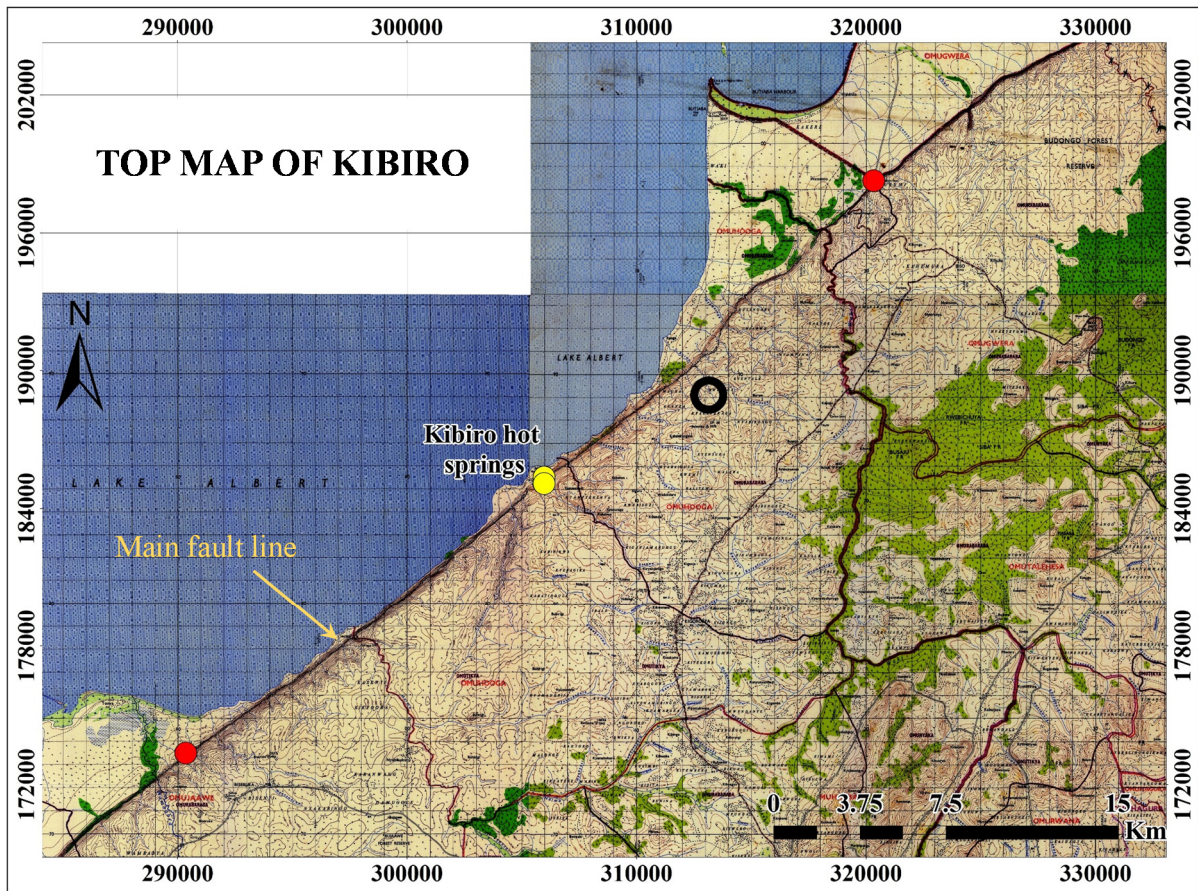
APPENDIX II: Comparison plots of calculated temperature results obtained from sixteen different equations of geothermometers for Öxarfjördur, Kibiro and Panyimur